WELL LOG ANALYSIS IN TABER MANNVILLE 'D' POOL,
TABER FIELD, ALBERTA, CANADA

A Thesis

Presented to the

Faculty of Graduate Studies and Research

of

The University of Manitoba

In Partial Fulfillment

of the requirements for the degree

Master of Science

by

S.M. Nazrul Islam

April, 1972

ABSTRACT

The Taber field is located to the south of the Taber rail station in the southern plains of the Province of Alberta, Canada. Thirty-eight well logs have been analysed for the evaluation of the Taber sand deposits of the Taber field Mannville 'D' pool. The oil reservoir is a fine- to medium-grained sandstone within shale formations of Lower Cretaceous age. The maximum reservoir thickness is 48 feet and the oil accumulation is found in sands of average porosity 18.9 per cent from 3,100 to 3,200 feet in depth.

The reservoir is in a stratigraphic trap formed by the pinching out of the sandstone. The accumulation of oil is probably controlled by porosity and permeability variations within the Taber sand. The Taber sand body, which is a separate and sealed reservoir, is lenticular in shape, surrounded by shales which may have been the source rock. An isopach map of the Taber sand discloses that the lens is approximately 14,000 feet long and has an average width of approximately 4,000 feet. The lenticular upper surface of the sand body, its relatively flat base and its excellent sorting suggest that the Taber member is a sand bar.

The producing area of the Taber Mannville 'D' pool is approximately 1,680 acres and the oil is produced by the use of natural reservoir pressure. The total recoverable oil reserves have been estimated by analysis of the well logs to be 4.80 million barrels out of 28.25 million barrels of oil in place. The crude oil is black and has a corrected gravity of 18.6° A.P.I.

ACKNOWLEDGEMENTS

The writer wishes to express his thanks to Dr. C.D. Anderson of the Department of Earth Sciences, University of Manitoba, for his supervision and advice throughout the study.

Thanks are due also to Dr. D.H. Hall of the Department of Earth Sciences, University of Manitoba, who originally suggested the thesis problem and contacted Chevron Standard Limited, Calgary, to provide the well log data. The author is grateful to Mr. W.S. Campbell and Mr. R.J. Flower of Chevron Standard Limited, who furnished the well log data, checked the results of the study, and made many useful suggestions. The technical assistance of Mr. W.G. MacLeod, Mr. W. Linke, and Mr. D. Pollard is also acknowledged.

The help and encouragement provided by Dr. W.C. Brisbin of the Department of Earth Sciences, University of Manitoba, is appreciated.

Financial assistance from the Government of Canada, External Aid Office, Ottawa, under the Technical Cooperation Scheme of the Colombo Plan enabled the author to pursue these studies at the University of Manitoba.

TABLE OF CONTENTS

LIST OF ILLUSTRATIONS

LIST OF SYMBOLS

F = Formation resistivity factor

R_w = Resistivity of formation water

R_{mf} = Resistivity of mud filtrate

$(R_w)_e$ = Equivalent formation water resistivity

$(R_{mf})_e$ = Equivalent mud filtrate resistivity

R_o = Resistivity of the formation 100% saturated with water

R_{xo} = Resistivity of flushed zone

R_t = True resistivity of the formation

SP = Spontaneous potential

SSP = Static SP

m = Cementation factor

n = Saturation exponent

ϕ = Porosity

S_w = Water saturation

κ = Permeability

Δt = Sonic transit time

Δt_{log} = Log derived sonic time

Δt_m = Sonic time of matrix

Δt_f = Sonic time of the fluid

ρ_b = Bulk density

ρ_m = Density of matrix

ρ_f = Density of the fluid

API = American Petroleum Institute

The glossary of terms used in well log analysis are adopted from Sheriff (1970).

CHAPTER I

INTRODUCTION

Location and Extent of the Area

The Taber field is located approximately one-half mile south of Taber rail station in the southern plains of the Province of Alberta, Canada, about 30 miles east of Lethbridge (Fig. 1). The Taber Mannville 'D' pool and other adjacent pools of Taber field are also shown in the figure. Logs of 31 oil wells and 7 dry wells covering an area of approximately 2,275 acres in Sections 18, 19, 20, 30, 31 and 32, Twp. 9, Rge. 16, W4Me were available for analysis.

Purpose and Scope

The purpose of the well log analyses for the Taber Mannville 'D' pool was to find out:

(i) the shape, extent, and possible origin of Taber sand deposits;

(ii) the relation, if any, between the sand deposits and the structure as represented by the top of

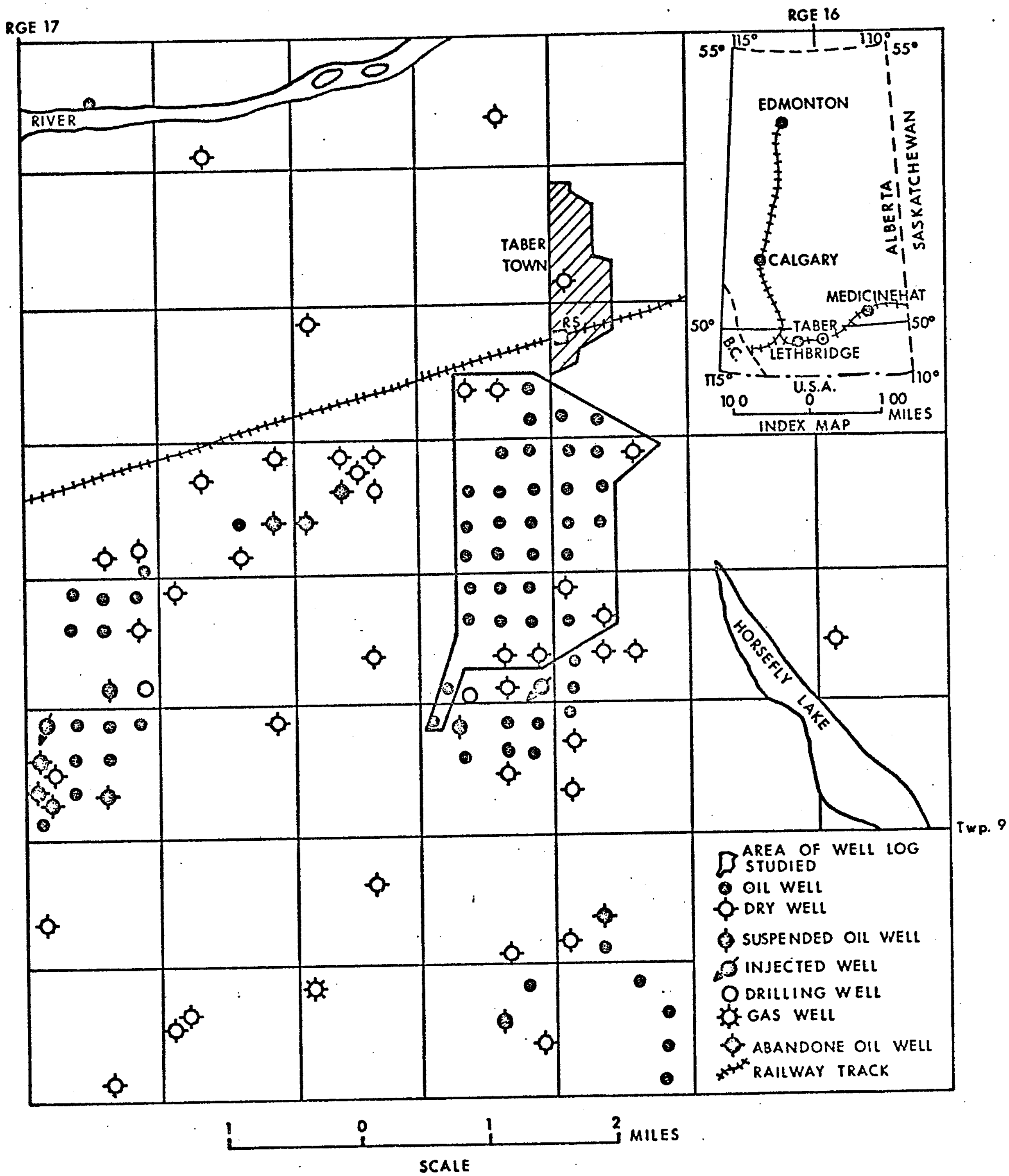

FIG·1 LOCATION MAP OF TABER OIL FIELD, TABER AREA, SOUTHERN ALBERTA PLAIN, ALBERTA, CANADA the Rierdon shale;

(iii) the relation between structure and accumulation of oil, and

(iv) to estimate the total recoverable oil.

Well logs, drill cutting information, and production data of each well were provided by Chevron Standard Limited, Calgary, during September, 1971. Many of the wells in this pool were drilled entirely through the Taber sand, and provided good control for stratigraphic correlation. Two core samples were made available at the Oil and Gas Conservation Board, Calgary, for detailed microscopic studies.

CHAPTER II

GENERAL GEOLOGY

Stratigraphy and Structure

The southern Alberta plain includes approximately 9,200 square miles of the Great Plains of Western Canada and is underlain by 6,000 to 13,000 feet of sediments, largely marine in origin (Fig. 2). The region is bounded on the west by the Rocky Mountains and on the east by the Precambrian Shield. The sedimentary section within this region contains sediments from earliest Paleozoic through the Mesozoic and Cenozoic with occurrence of important gaps.

Several reports on the geology of the southern Alberta plains have been published by the Geological Survey of Canada. Russell and Landes (1940), Hage and Hume (1941), Glaister (1959), Andrichuk (1970), and many other authors made significant contributions towards the detailed geologic description of the area. General references to petroleum deposits, their environment and origin may be best found in Hume (1928), Cheyney (1948), Lowenstam (1948), Robert (1948), Landes (1951), and Levorsen (1954).

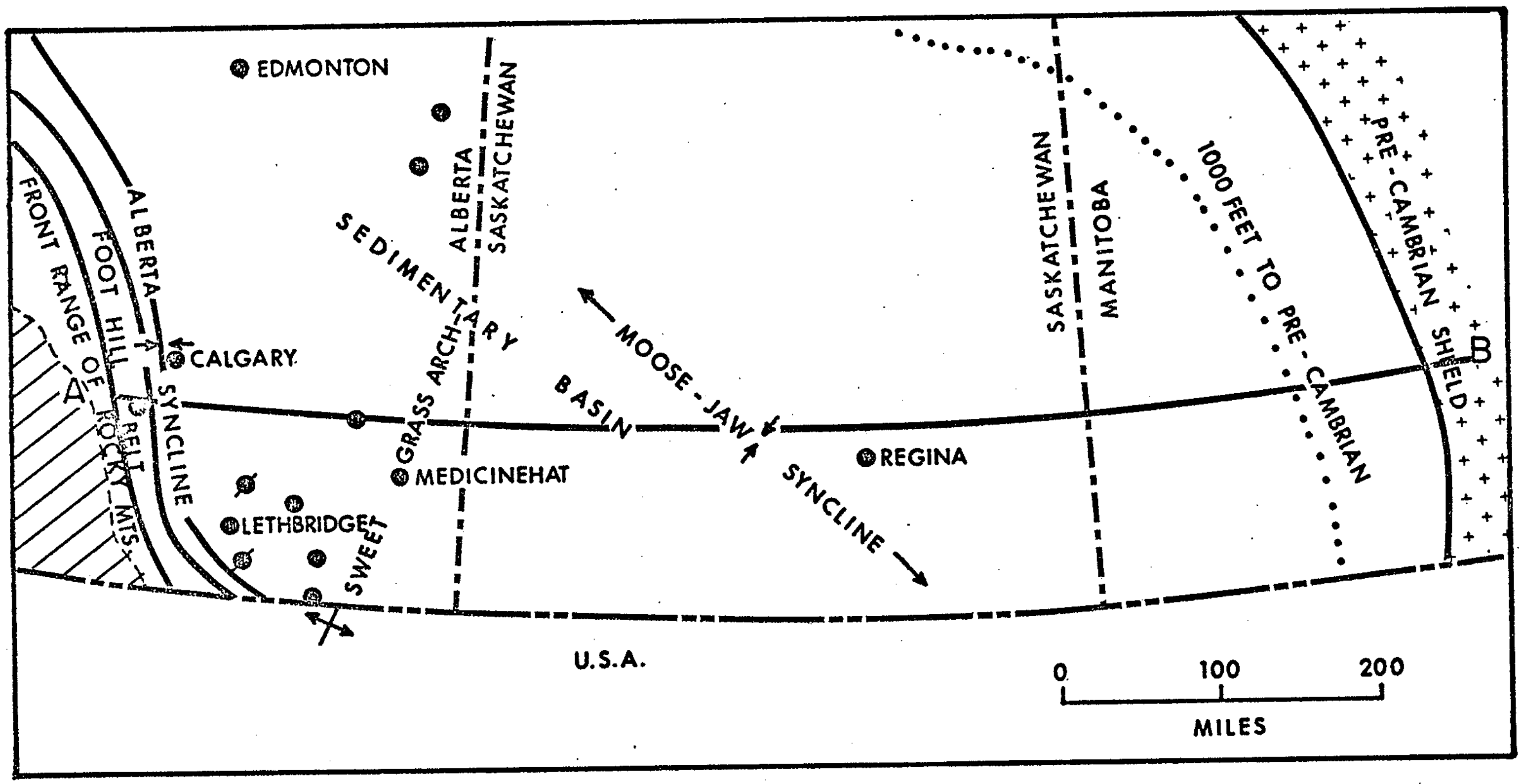

FIG. 2 MAP SHOWING GENERAL FEATURES OF WESTERN CANADA

(FROM A.A.P.G. - 1941)

Stratigraphy

The general stratigraphic sequences of the southern plains of Alberta is summarized in Appendix I.

Cambrian to Lower Cretaceous

Cambrian to Lower Cretaceous rocks do not outcrop anywhere on the plains of southern Alberta and are known only from well borings (Russell and Landes, 1940). From the very limited data it has been indicated that the thickness of the Cambrian and Devonian strata, predominantly limestone, dolomite, and shale, is about 1,500 feet. The Mississippian strata consist of about 1,000 feet of mostly limestone. Ordovician, Silurian, Permian and Triassic rocks are absent beneath the southern Alberta plains. The thickness of the Jurassic strata, predominantly shale and limestone, ranges from 150 to over 250 feet. The thickness of the Lower Cretaceous strata, predominantly shale and sandstone ranges from 250 to 650 feet. The Mannville Group, dominantly non marine and the marine Bow Island Formation are the two major lithologic units of the Lower Cretaceous strata in the southern part of Alberta (Glaister, 1959). The Mannville Group overlies the marine Jurassic shale unconformably and usually contains a basal quartzose sandstone member called the Cutbunk, Sunburst and Taber sandstones in southern Alberta. The thickness variations of Jurassic and Lower Cretaceous strata were established from drill hole results (Russell and

Landes, 1940).

Upper Cretaceous

The area of exposure of the older Upper Cretaceous rocks is limited to the extreme southern part of the Alberta plain. The Pakowki, Foremost, Old Man, Bear Paw, Blood-reserve, St. Mary, Eastend and White Mud Formations (Appendix I) are well exposed in different areas of the southern Alberta plains. The Upper Cretaceous rocks consist of predominantly shale, sand, clay, and bentonite. The thickness of individual formations ranges from a few feet to a few hundred feet.

Tertiary

The Willow Creek beds of Paleocene age are confined to the extreme southwestern corner of the region and outcrop on the north branch of the Milk River. The Ravenscrag Formation of Upper Paleocene is best exposed and confined to the Cypress Hills district in southeastern Alberta. The Cypress Hills Formation of Oligocene age outcrops at several points near the Saskatchewan-Alberta border. The tertiary rock consists of clay, sandstone, gravel and conglomerate, etc.

Quaternary

A mantle of unconsolidated materials of Pleistocene and Recent age, consisting generally of glacial till, outwash, gravel, sand and silt, covers the whole of the southern plains of Alberta with the exception of the tops of some of the higher plateaus, such as the Cypress Hills.

Structure

Figure 3 shows an east-west vertical section through the Alberta plains. The structure is an asymmetric trough whose axis lies immediately east of the foothills in southern Alberta, but diverges eastward farther to the north. The sedimentary section as a whole thickens gradually from east to west across the plains and foothills, and in the case of certain formations, very great thickening occurs in the front ranges of the mountains and farther west. It is generally accepted that the axis of the geosyncline, beginning in Precambrian time when it lay west of the present site of the Rockies, underwent progressive shifting eastward until the basin was finally destroyed by the Laramide revolution (Levorsen, 1941).

Along the western margin of the plains the dips increase to between 50 and 100 feet to the mile, and this continues to the axis of the Alberta syncline, which lies west of the area (Russell and Landes, 1940). Subsidiary folds also occur on the flanks of the Alberta syncline, most of them having a trend that parallels the axis of the main structure.

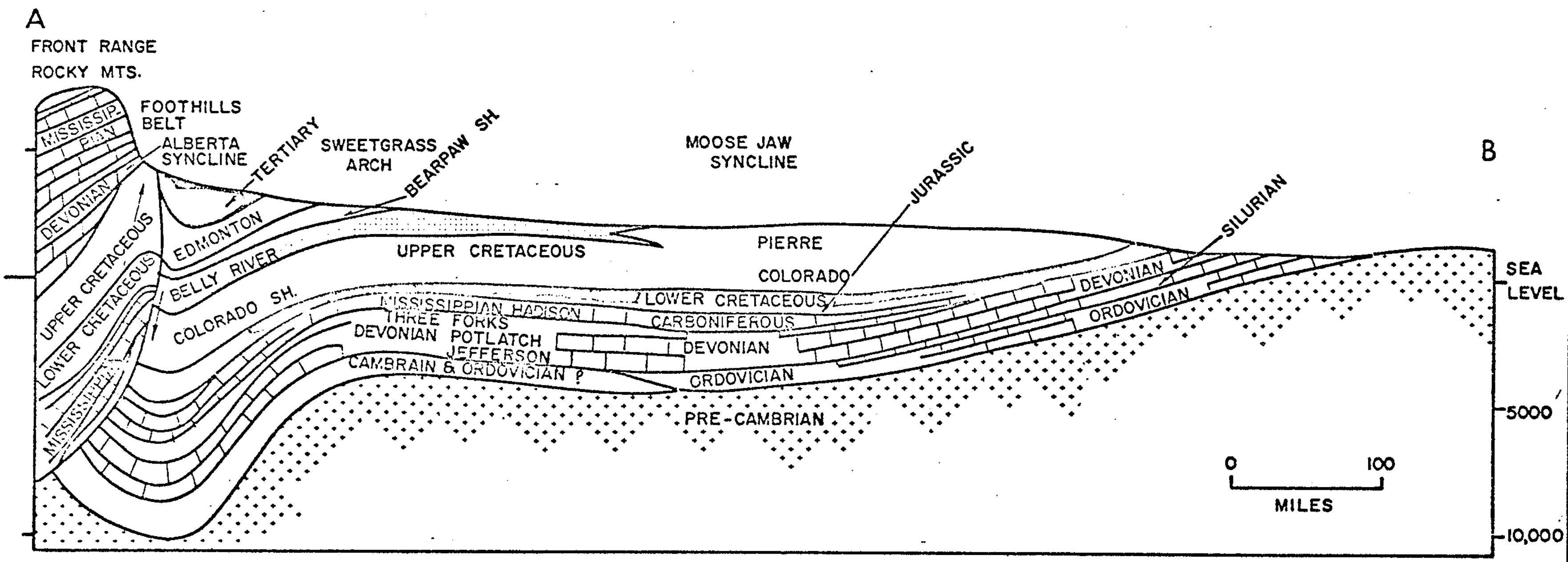

TRUE SCALE

WESTERN CANADA

FIG. 3 GENERALIZED STRUCTURE SECTION ACROSS SOUTHERN PLAINS REGION OF WESTERN CANADA. LOCATION OF SECTION SHOWEN IN FIGURE 2.

(FROM A.A.P.G. - 1941)

CHAPTER III

TABER OIL FIELD

The Taber field is situated in Twps. 9 and 10, Rges. 16 and 17, W4M about 30 miles east of Lethbridge and contains a number of hydrocarbon pools. The traps containing the hydrocarbon pools are due to the closed local structures, to lenticular pinch outs across plunging structures and to isolated zones of porosity and permeability. The field is included in area which has many shows of oil at depths ranging from 3100 to 3300 feet in the lower Cretaceous Blairmore Formation. The discovery well for the area was Plains Petroleum Corporation No. 2 well in Lsd. 11, Sec. 25, Twp. 9, Rge. 17, W4M, which was completed and brought on production in October, 1937. This well proved to have a very short production life and was a non-commercial discovery. In June, 1942, Standard Oil Company of British Columbia completed its Taber Province No. 1 well in Lsd. 9, Sec. 18, Twp. 9, Rge. 16, W4M as the discovery well of the East Taber pool. Subsequent drilling outlined an area of 280 acres containing eight producing wells. The Taber Mannville 'D' pool (Fig. 1) is located on the north side of this pool. The first producing well of this pool in Lsd. 1, Sec. 31, Twp. 9, Rge. 16, W4M, was completed in July, 1966 by Sprux Dalex Company. Later on the pool was developed by extensive drilling operations by different oil companies during the years 1967 and 1968. The pool has now thirty-one producing wells and seven dry wells which outline an area of 1680 acres approximately. The most recent producing well in Lsd, 4, Sec. 19, Twp. 9, Rge. 16, W4M was drilled up to a depth of 3276 feet in October, 1971 by Chevron Standard Limited. The average oil pay thickness of this pool is 22 feet and maximum reservoir thickness is 48 feet. The oil has a gravity of 18.6° API. In August, 1944, Standard Oil Company of B.C. Nassau Exploration Taber Province 87-15-A in Lsd. 13, Sec. 15, Twp. 9, Rge. 17, W4M encountered 22° API gravity oil in a basal Cretaceous sand and placed on production as the discovery well of the West Taber Field. This pool covers an area of about 480 acres and 15 wells have encountered production. The oil of this pool has a gravity of 22° API.

CHAPTER IV

WELL LOGGING

Spontaneous potential (SP), electrical induction, caliper, gamma ray, sonic and density logs were available for analyses of the Taber Mannville 'D' pool. These six types of well logs are shown in Fig. 4 and they are discussed separately in the following sections. The types of logs available for each well is given in the Appendix IV. The principle, equipment and uses of these logs are available in Schlumberger Well Survey Corporation Documents (1958 and 1969), Kokesh and Blizard (1959), Pickell and Heacock (1960), Tixier, Alger and Tanguy (1960) and Moran and Kunz (1962). Suggestions for better and improved log interpretation by Doll and Martin (1960), log interpretation in sandstone by Wyllie (1960), formation evaluation by Lynch (1962), and geologic well log analysis by Pirson (1970) are worth mentioning.

Spontaneous Potential (SP) in Borehole

The SP log is a record of naturally occurring potential differences between a surface electrode and a movable electrode in the borehole. It is generally

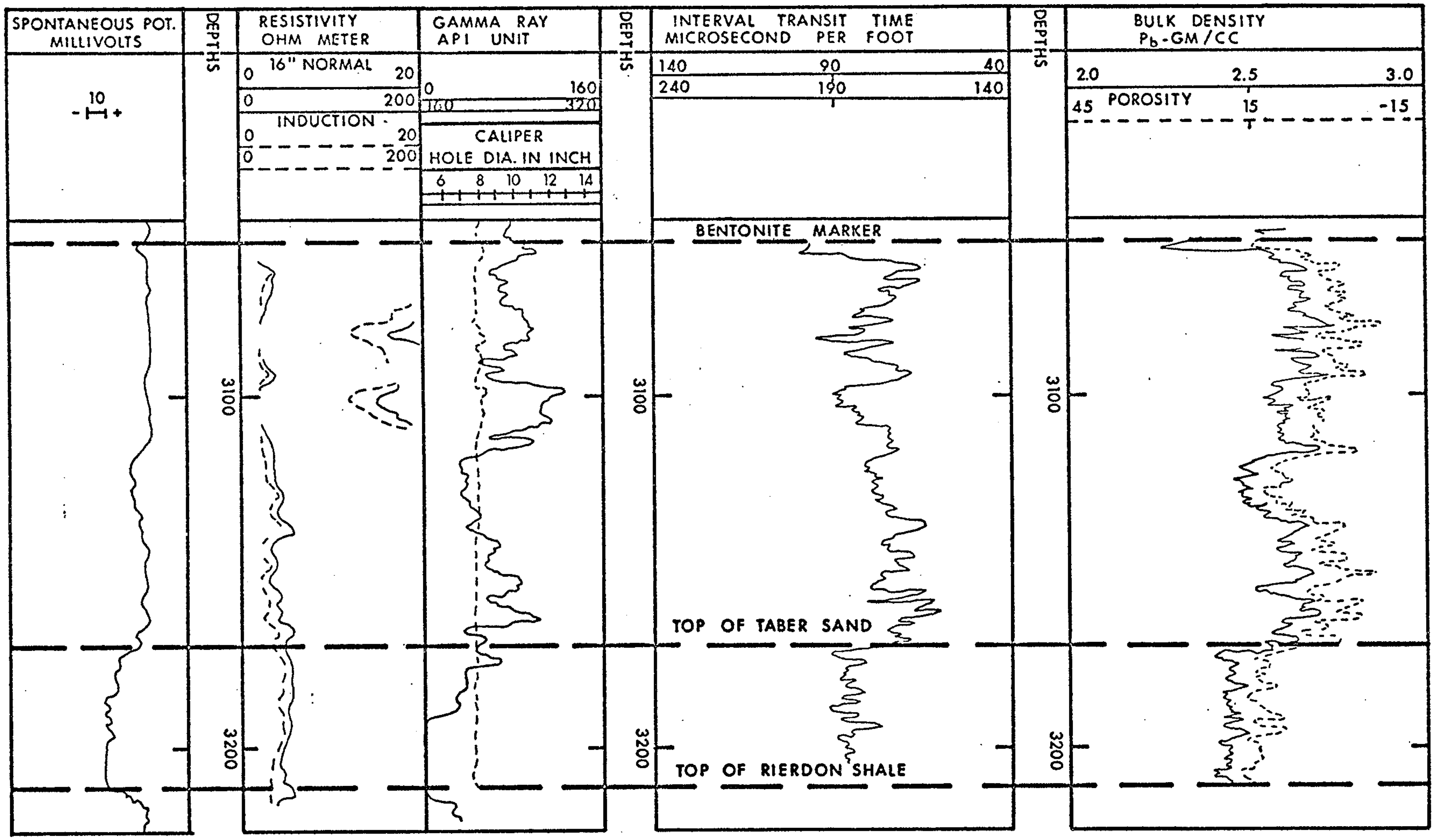

FIG. 4 SIX TYPES OF LOGS, TABER MANNVILLE 'D' POOL, TABER FIELD, ALBERTA, CANADA

recorded on Track I of the log, usually in conjunction with resistivity surveys. The SP curve of higher potential at the base of the Taber sand is shown in Fig. 5.

Origin of the SP

The electromotive force which generates the SP currents within the borehole are considered to be the results of electrochemical and electrokinetic phenomena.

The electric currents caused by electromotive forces of electrochemical origin occur at the contacts between the drilling mud (or its filtrate) and the formation water in the pores of the permeable bed, and across the adjacent shales. The electrochemical potential results from the solution-concentration difference between the drilling mud and the formation water. Cations and anions have considerable mobility in shale; Na^+ cations move through the shale from the more concentrated to the less concentrated solution. This movement of charged ions constitutes an electric current and gives rise to an electrical potential across the shale.

The second possible cause of spontaneous electric potential caused by the electro-filtration is considered electrokinetic in nature. Filtration of mud through the mud cake may cause an electromotive force. The forces may appear primarily where the pressure difference of the mud is greater than the pressure in the formation. The flow of the mud filtrate from the well into the formation may

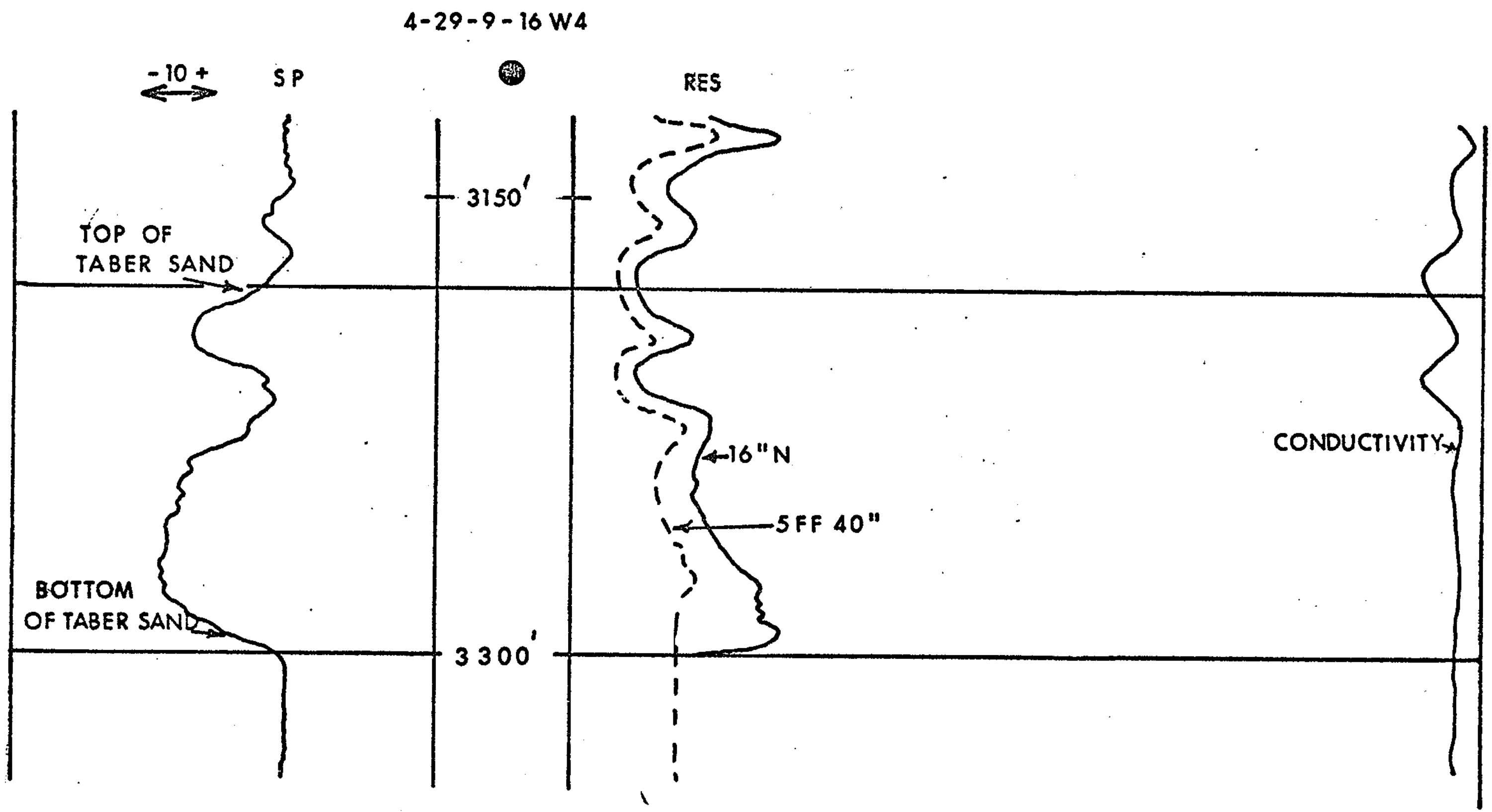

FIG. 5 SP CURVE OF HIGHER POTENTIAL AT THE BASE OF THE TABER SAND.

produce a negative potential.

Equipment

The equipment for recording SP log within the borehole consists of two electrodes, recording galvanometer and one cable, etc. The electrodes are made of relatively stable material - lead - and any constant potential difference between the surface electrode and one in the hole may be balanced out by an adjustable voltage from a potentiometer circuit. The SP sensitivity scale is chosen and the shale - base - line position is set by the engineer running the log so that SP curve deflections remain in the SP track. The measurement is expressed in millivolts, starting from a base line near the centre of the record.

Determination of R_w from the SP Log

The formation water resistivity R_w was determined from the SP curve on trial basis just to compare the results obtained from oil base core analyses using the formula

$$SSP = -K \log \frac{(R_w)_e}{(R_{mf})_e}$$

where K varies in direct proportion to absolute temperature and $(R_w)_e$ and $(R_{mf})_e$ are the equivalent resistivities of formation water and mud filtrate respectively. The graphical representation of this formula is given in Schlumberger Log Interpretation Chart - 1969, page 10. An example of R_w determination is given below:

Well location in Lsd. 13, Sec. 20, Twp. 9, Rge. 16, W4M (See Fig. 22).

Given values

R_{mf} = 2.6 ohm-meters at 60°F

Bottom hole temperature = 90° F at 3276 feet

Observed values

SSP = -55 mv at 3150 feet at formation temp. 88°F

Calculated values

R_{mf} = 2.2 ohm-meters at 88°F

and $(R_{mf})_e$ = 2.2 x 0.85 ohm-meters

= 1.86 ohm-meters (in case of R_{mf} at 75°F is greater than 0.1 ohm-meter)

Thus

$$\frac{(R_{mf})_e}{(R_w)_e} = 6.0$$

therefore $(R_w)_e = \frac{1.86}{6.0} = 0.31$ ohm-meters

and R_w = 0.35 ohm-meters found from the chart

The above calculations were made using three charts Nos. Gen-9, SP-1 and SP-2, Schlumberger Log Interpretation Chart - 1969.

The SP anomaly in this particular well was chosen to derive R_w because of the fact that the SP anomaly was thoughtto be relatively less influenced by the shale streak within the reservoir rock. However using the SP curve is probably the poorest method of getting R_w when the horizon is not a clean thick water-bearing formation.

After careful study of 30 samples from six southern Alberta oil fields by Atomic Absorption Spectroscopy (AAS), MacLeod (1970) concludes that even though there was a considerable variation in ion composition of the formation waters, the reservoirs are continuous and the variance represents a dilution by fresh water influx along the Sweet Grass Arch. Results of the chemical analyses of one of the samples collected from the well in Lsd. 4, Sec. 19, Twp. 9, Rge. 16, W4M are shown in Table I.

The elemental analyses of formation water obtained from different wells in Taber field indicate that the upper formation water is more saline and lesser resistive than the bottom water which may have been flushed by fresh water encroachment along the Sweet Grass Arch. The resistivity R_w of irreducible water which clings to the grains of the rock within oil bearing interval and cannot be displaced are evaluated from the oil base core of well in Lsd. 12, Sec. 29, Twp. 9, Rge. 16, W4M (Fig. 22) and it has been found that its resistivity is much lesser than the bottom water resistivity. The formula used for R_w measurement from this particular oil base core is given below

$$S_w = \sqrt{\frac{1}{\phi^2} \frac{R_w}{R_t}}$$

$$R_w = S_w{}^2 \cdot R_t \cdot \phi^2$$

Table I. Results of the water sample analysis of well in Lsd. 4, Sec. 19, Twp. 9, Rge. 16, W4Me (see Figure 22), Taber Mannville 'D' pool, Taber Field, Alberta, Canada. (Adapted from Core Laboratories-Canada Ltd. - 1971).

Formation - Taber sand	Interval - 3165' - 3216'
Resistivity - 1.24 ohm.-meters @ 72°F	Cal. Tot. Solid - 7.267 mg/liter
Specific Gravity - 1.9948 @ 60°F	By Evaporation @ 110°C
pH - 8.2 H S - absent	By Evaporation @ 180°C
Refractive Index - 1.3334 @ 73°F	At Ignition

Na+K	Ca	Mg	Fe	Ba	Br	I	Cl	HCO_3	SO_4	CO_3	OH
Milligrams Per Litre											
2180	65	17	*pres.	-	-	-	1461	3514	30	nil	nil
Per Cent Calculated Solids											
30.0	0.9	0.2	*pres.	-	-	-	20.1	48.4	0.4	0.0	0.0
Meq Per Liter											
94.8	3.2	1.4	*pres.	-	-	-	41.2	57.6	0.6	0.0	0.0

* Total iron = 0.20 gm/liter.

An average water saturation of 32 p.c., average porosity 17.3 p.c. were established by laboratory measurements on this particular oil base core and the formation resistivity of 50 ohm-meters was derived from 40" induction electrical log. Applying all these values into the above formula, R_w was found to be 0.15 ohm-meters. This value was used for evaluation of hydrocarbon fluid in Taber Mannville 'D' pool.

Recognition of Significant Geologic Features on the SP Logs

Three significant geologic features have been recognized on the SP logs such as unconformity, facies and time marker.

Unconformity - the known bed sequences of Taber sand suddenly disappear on SP logs.

Facies - interbedded sands and shales within the sand reservoirs represents a littoral environment.

Time marker - a thin bentonite bed is recognized on SP logs by a single peak of low potential.

Correlation

The reference marker used to establish the position of the top of the Taber sand is a bentonite marker. With induction logs, the bentonite streak appears as a single deflection on the SP log and has been easily recognized on every SP log (Figs. 6 and 7). Since the sediments above the bentonite marker are assumed to be horizontal, the marker bed has been drawn horizontally in Figure 6 and 7 and top and bottom of the Taber sand have been correlated from log to log with reference to this time marker. This establishes a sedimentary paleo-sand distribution within the Taber Mannville 'D' pool. The structural deformation is then restored from topographic subsea level contours on the marker bed (Figs. 8 and 9).

Induction Electrical Log

The induction electrical log can be run in holes filled with conductive muds as well with non-conductive muds. Logging devices are focussed in order to minimize the influence of the borehole and of the surrounding formation. They are also designed for deep investigation and reduction of the influence of the invaded zone.

Principle

Practical induction sondes include a system of several co-axial transmitter and receiver coils. A sonde with one transmitter and one receiver coil is shown in Fig. 10. The transmitter coil is energized by a 20 kc oscillator and the alternating magnetic field thus created induces secondary currents in the formations. These currents flow in circular ground-loop paths co-axial with

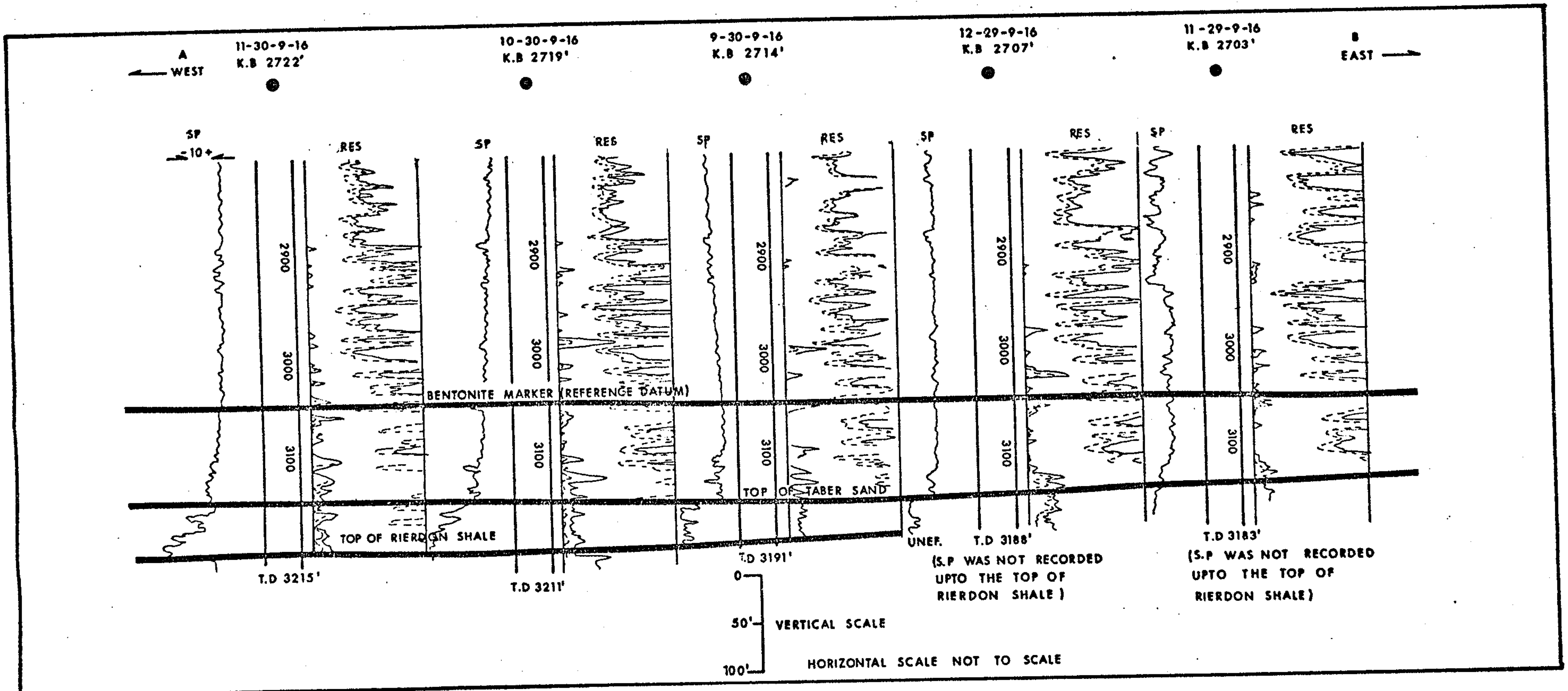

FIG. 6 EXAMPLE OF ELECTRIC LOG CORRELATION FOR DELINEATION OF TABER SAND STRATIGRAPHIC TRAP ACROSS A-B (SEE FIG.24)
TABER NORTH D POOL, TABER FIELD, ALBERTA, CANADA

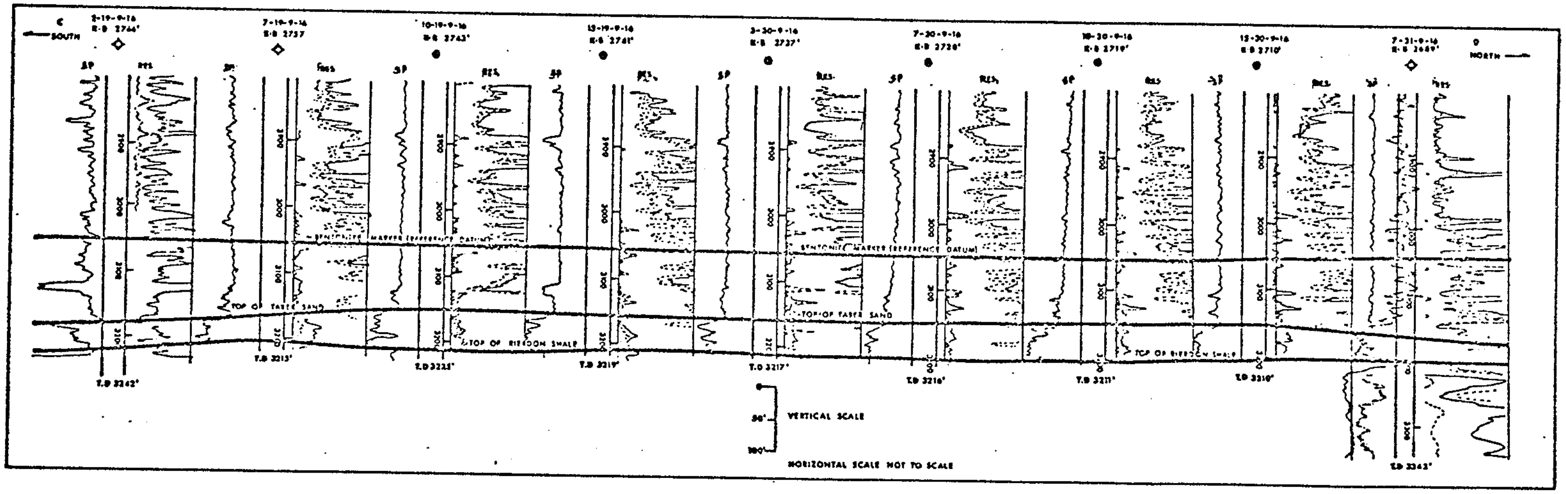

FIG. 7 EXAMPLE OF ELECTRICAL LOG CORRELATION FOR DELINEATION OF TABER SAND STRATIGRAPHIC TRAP ACROSS C-D (SEE FIG.24)
TABER NORTH D POOL, TABER FIELD, ALBERTA, CANADA

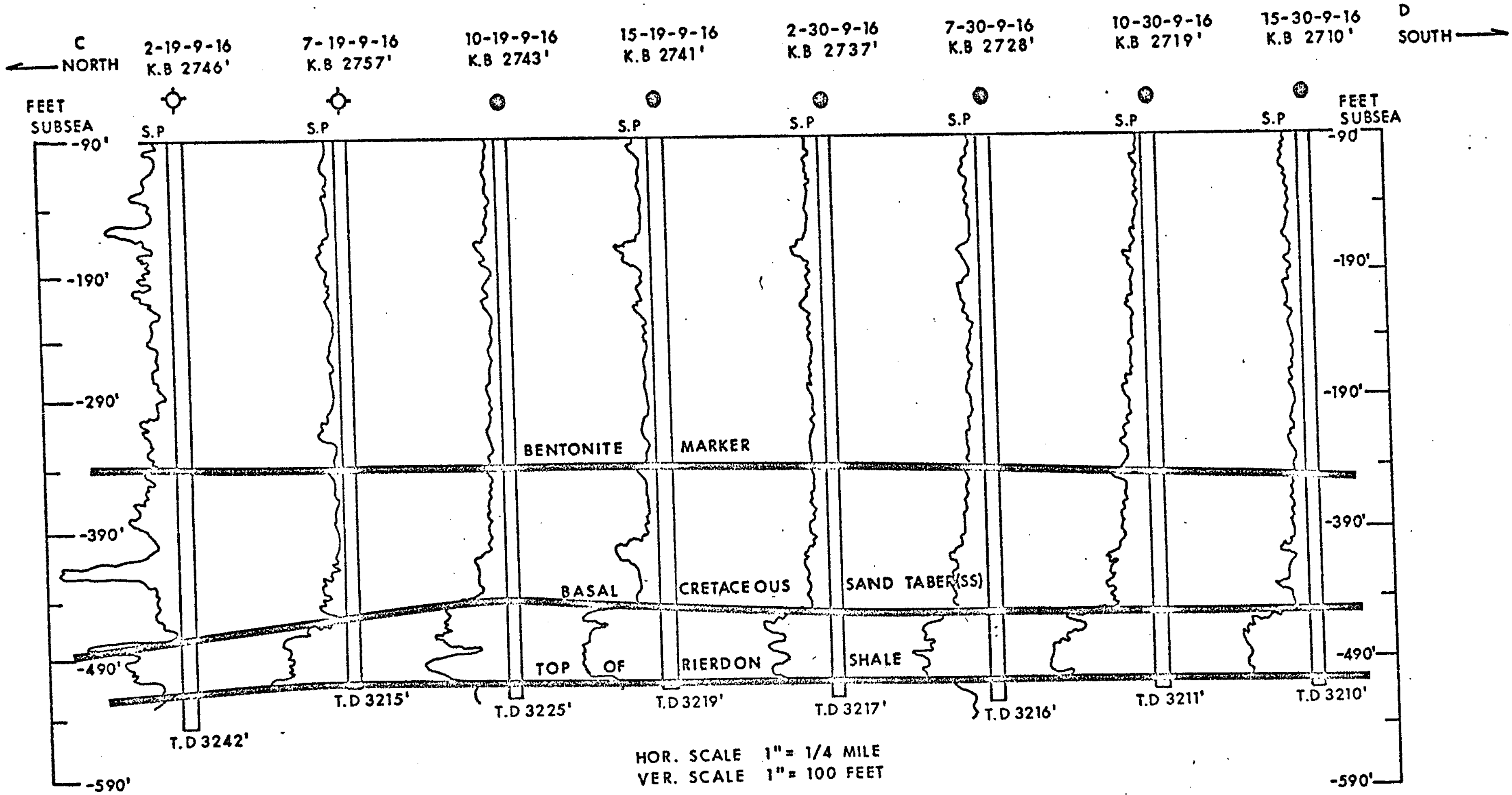

FIG. 8 NORTH-SOUTH CROSS SECTION OF THREE HORIZONS ACROSS PROFILE C-D (SEE FIG 24)

TABER MANNVILE POOL, TABER FIELD, ALBERTA

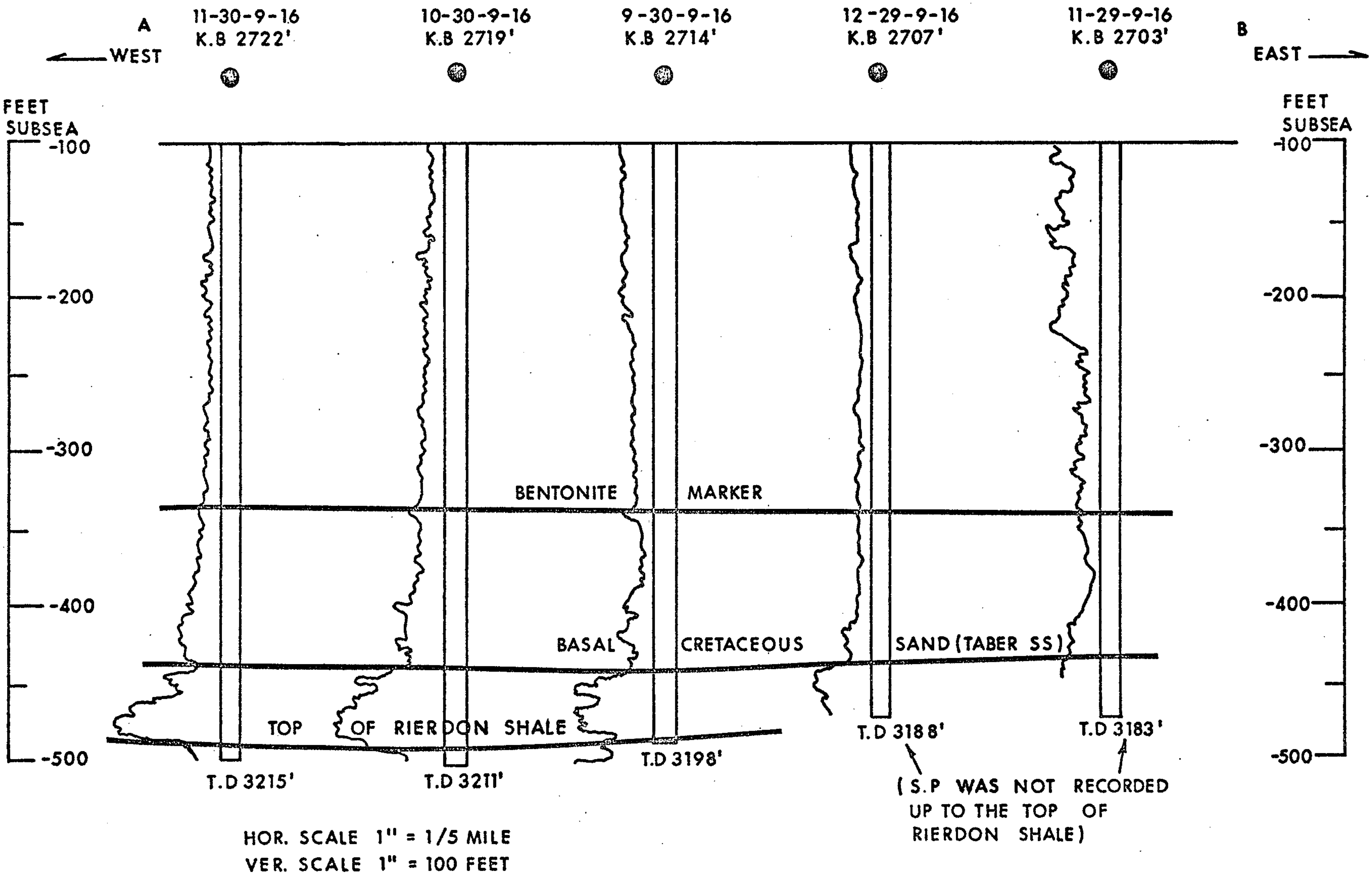

FIG.9 WEST-EAST CROSS SECTIONS OF THREE HORIZONS ACROSS PROFILE A-B (SEE FIG.24)

TABER NORTH D POOL, TABER FIELD, ALBERTA

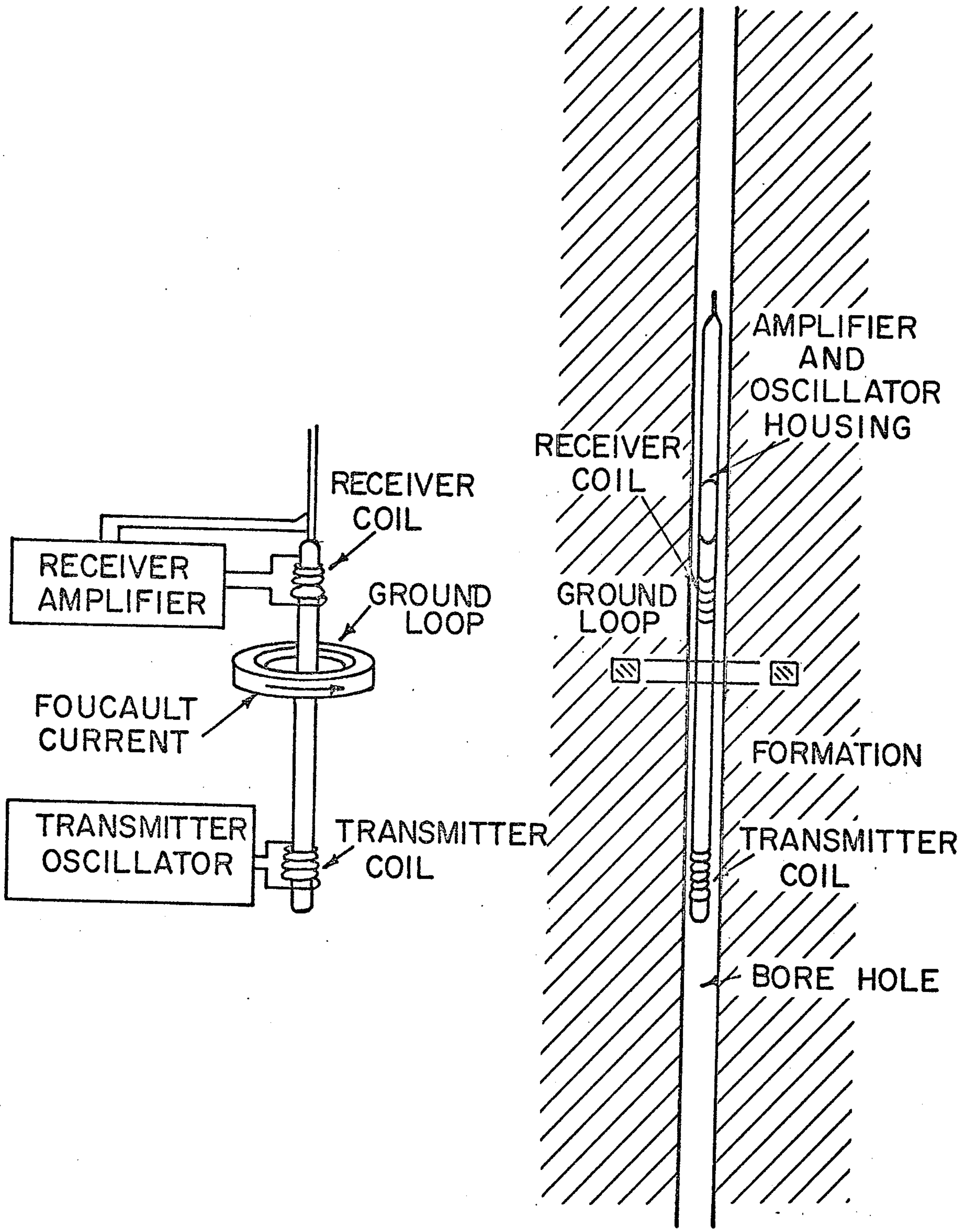

FIG.10 SCHEMATIC OF TWO-COIL INDUCTION SONDE.
COURTESY SCHLUMBERGER.

the transmitter coil. These ground loop path currents, in turn, create oscillation magnetic fields which include signals in the receiver coils. The receiver signals are essentially proportional to the conductivity of the formations.

Equipment

The Induction-Electrical Survey (I-ES) tool consists of a 16" normal device and an SP electrode, a deep investifation 6FF40 or a medium investigation 5FF40 Induction configuration.

In the 16" normal device a current of constant intensity is passed between two current electrodes and the resultant potential difference is measured between two potential electrodes. The distance between one current electrode and one potential electrode both lowered within the hole is kept 16". In the induction focussing system both 5FF40 and 6FF40 tools have a main coil spacing of 40". The 6FF40 tools receives greater percentage of its signal than 5FF40 in the case of deep investigation around the borehole. The conductivity measured either with 5FF40 or 6FF40 tools is recorded in Track 3. In Track 2 both the 16" normal and reciprocal induction curves are recorded on the same linear scale. The linear scale is in ohms per meter increasing to the right. Figure 5 illustrates the presentation of I-ES log within the Taber sand.

Determination of R_t

In Taber Mannville 'D' pool, the sands are dirty and the contrast between the resistivities of water- bearing sands and oil-bearing sands is not very great. The oil-bearing formation contains a large amount of interstitial water. S_w is estimated 40 p.c. and R_t is expected lower than R_{xo}. R_{mf} is greater than R_w and accordingly the resistivity of the invaded zone is higher than the true resistivity of the formation. In this particular case, most of the induced currents tend to flow in the uncontaminated zone and the contribution of this latter to the total signal is large and thus 40" induction log has been used with confidence as a close approximation to R_t.

Empirical Relation between Resistivity, Porosity, and Water Saturation

In an experimental investigation of a large number of water-saturation clean sandstones, Archie (1942) found that the resistivities of sandstone and the water could be related by the equation

$$R_o = FR_w$$

where F is a constant for a particular sandstone sample. The constant is called the formation resistivity factor. Further investigation by Archie established that F is a function of porosity. According to him satisfactory results are obtained with $F = \frac{1}{\phi^2}$ in compacted sands. The Taber sand contains oil and water, the resistivity R_t is a function not only of F, but also of the water saturation S_w. Archie (1942) determined experimentally that the water saturation of a clean formation can be expressed in terms of true resistivity R_t as

$$S_w{}^n = \frac{FR_w}{R_t}$$

where n is the saturation exponent, is generally taken equal to 2. The formula used for determining water saturation S_w in Taber sand was thus derived from the above equation as

$$S_w = \sqrt{\frac{FR_w}{R_t}} = \sqrt{\frac{1}{\phi^2}\,\frac{R_w}{R_t}}$$

Caliper Log

The caliper log is a measurement of the size of the borehole. The log was run inconjunction with the gamma ray log in Track 1 (Fig. 11), which shows the size and condition of the borehole. The instrument recorded hole diameter up to 8" in some wells in the Taber sand. The size of the bit used for drilling varies from 6¼" to 7-7/8".

Principle

Figure 12 is a schematic drawing of the section gauge caliper log. On the body of the instrument are

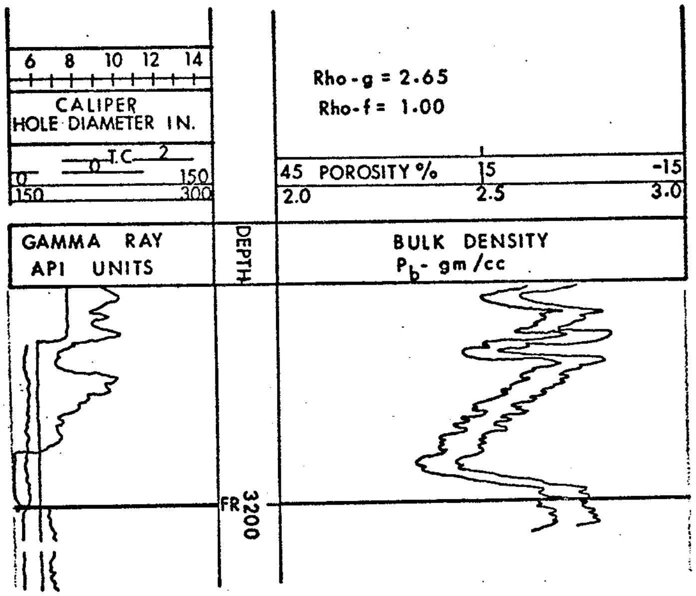

FIG.11 CALIPER AND GAMMA RAY CURVE IN TABER SAND

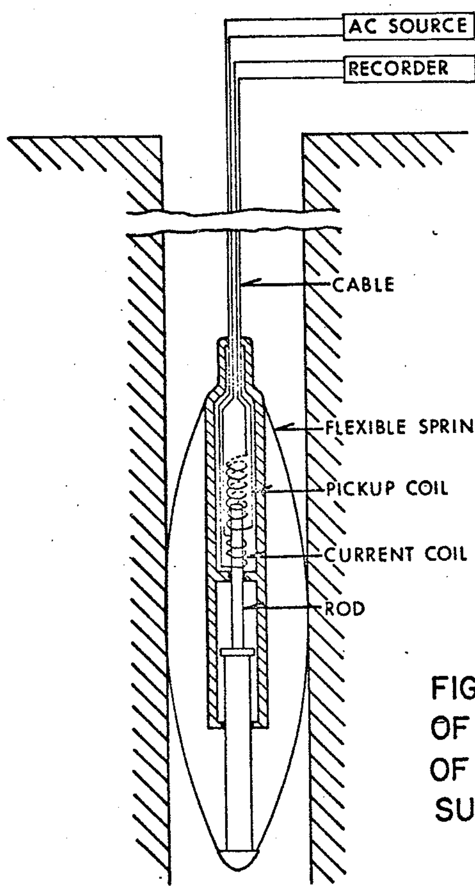

FIG.12 SCHEMATIC DRAWING OF A SECTION GAGE. (COURTESY OF SCHLUMBERGER WELL SURVEYING CORPORATION)

fastened three large flexible springs which ride against the wall of the borehole. These three springs are attached to a movable rod at the bottom of the tool. The position of this rod in the tool body is governed by the size of the hole. The position of the rod also governs the amount of the inductive coupling between the current coil and the pick up coil in the tool body. Changes in the borehole size are therefore reflected in changes in the voltage induced in the pick up coil and these voltages are logged at the surface.

Equipment

Two types of instruments are used in the field, the conventional section gauge and the microcaliper. The conventional section gauge was recorded in Track 1 in conjunction with the gamma ray log in the borehole penetrating the Taber sand.

Uses

Caliper log was essentially used by the drilling engineer to calculate the amount of cement necessary to fill up the annular space between the casing and the well and to select packer seats.

Gamma Ray Log

Gamma ray log measures the natural radioactivity of the formation. A few radioactive elements, such as uranium, thorium and potassium emit gamma rays spontaneously. Within the Taber sand gamma ray logs reflect the shale content of the formation (Fig. 11) because shale contains more radioactive elements than the clean sand. This log is principally used to distinguish between shales and non-shales within the sand reservoir.

Principle of the Instrument

The principle of the instrument used in gamma ray logging is illustrated in Fig. 13. A gamma ray entering the thallium-activated sodium iodite crystal interacts with electrons in the crystal and produces a flash of light. This light in turn strikes the sensitive surface of the photocathode giving rise to an electrical signal. The extremely short duration of light flashes permits a high counting rate. The intensity of the electrical signal is proportional to the energy of the incident gamma ray. This proportionality makes it possible to count only those incident rays of a given wavelength by electronically separating only those pulses of a selected amplitude.

Equipment

Scintillation counters are now generally used to measure radioactivities in boreholes. They are much more efficient than Geiger-Muller counters, which were previously used.

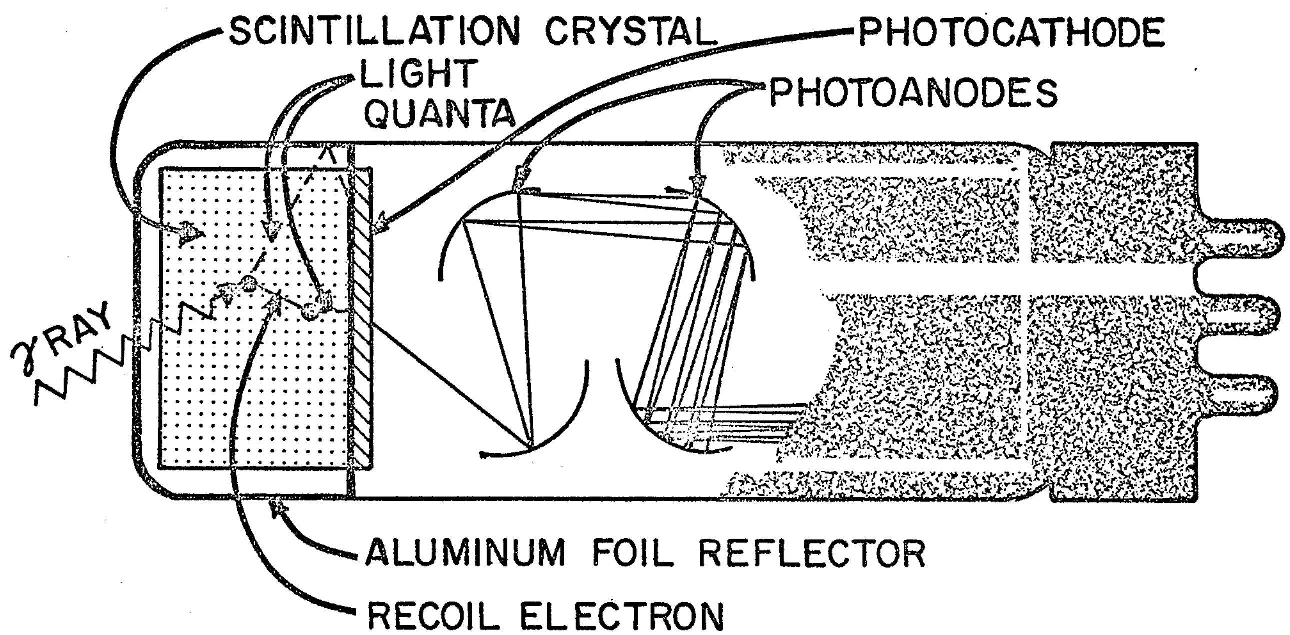

FIG.13 SCHEMATIC ILLUSTRATION OF A SCINTILLATION COUNTER. (FROM LYNCH)

The Unit of Radioactivity

The gamma ray logs were calibrated in API units. The API (1959) established an empirical calibration standard at the Nuclear Logging Calibration Facility, University of Houston, Houston, Texas. In Taber sand 32° API units were used as shale cut off for quantitative estimation of sand.

Shape of the Curve at Interface

Figure 11 shows an example of gamma ray log and SP curve recorded in same series of sands and shales. The SP curve gives qualitative indication of shale within the Taber sand. The demarcation of clean sand and the evolution of shale within the reservoir rock have been made possible using gamma ray logs as shown in Fig. 11.

Application of Gamma Ray Log

The numerous fluctuations of the gamma ray curve recorded in the borehole of Taber Mannville 'D' pool gave a much more detailed picture of the variation in shale content of the Taber sand than did the SP curve. Gamma ray was primarily used for quantitative evaluation of shale content within the reservoir rock.

Sonic Log

The sonic log is a continuous record of the time for a compressional sound wave to traverse one foot of formation. The rate of propogation of the compression wave through a porous rock depends on the clastic properties of the rock matrix and its contained fluids. Since the subsurface lithology is known, the sonic time is used for porosity determinations. A relation between sonic time and core measured porosity has been established.

Principle

A schematic drawing of sonic logging sonde is shown in Fig. 14 for two transmitter-receiver sets. Contained within the sonde is instrumentation for transmitting information to the surface and the timer which controls the rate of generation of sound impulses. The transmitters are pulsed alternatively and Δt values are read on alternate pairs of receivers. The Δt values from the two sets of receivers are averaged automatically by a computer at the surface.

Equipment

The sonic tools used are of BHC (borehole compensated) type. This type sonde eliminates spurious effects as well as errors due to sonde tilt (Kokesh and Blizard, 1959).

Log Presentation

The interval transit time, Δt, has been recorded on a linear scale in Tracks 2 and 3 of the log (Fig. 4). A 3-arm caliper curve and a gamma ray curve have also been

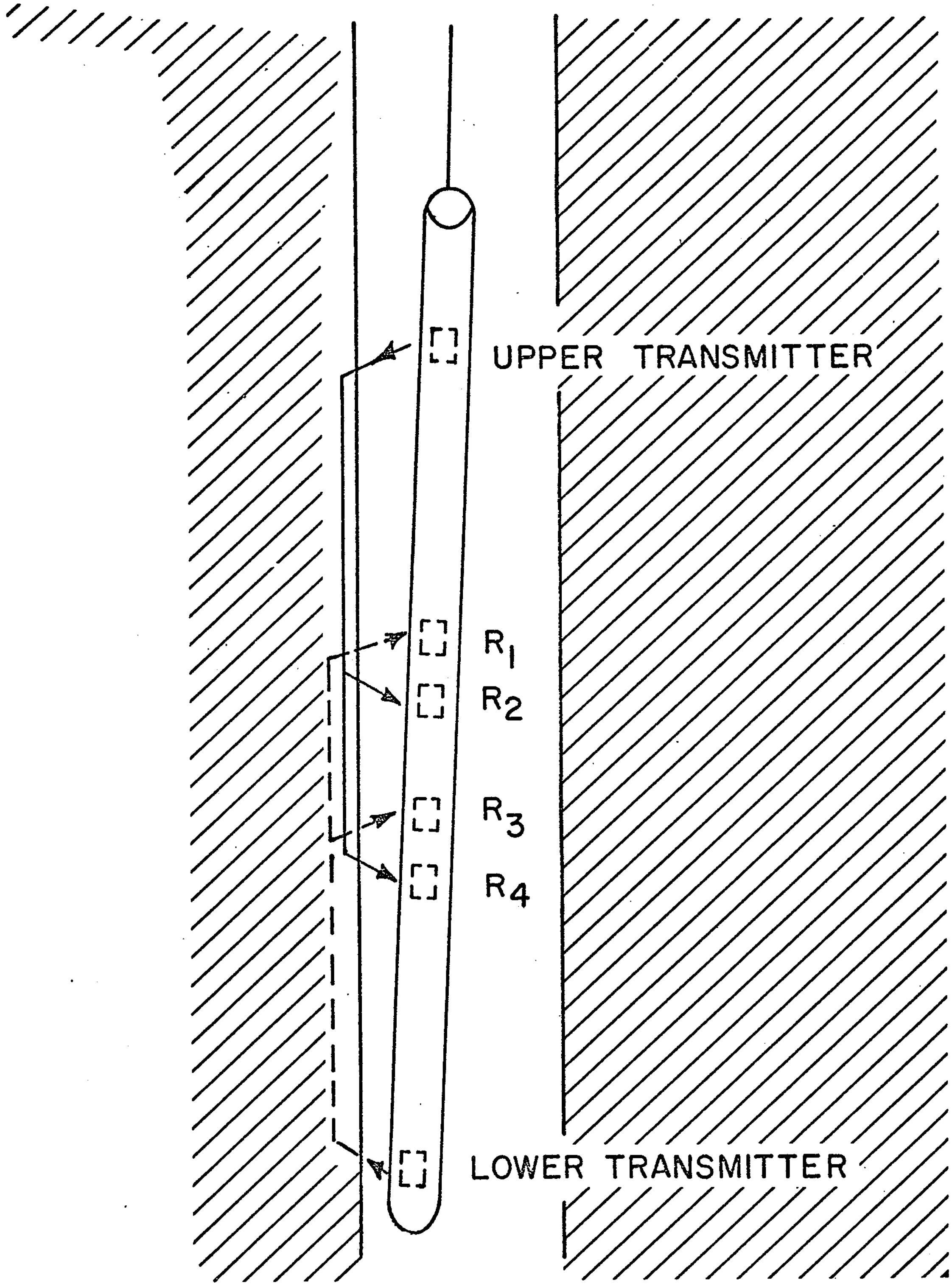

FIG.14 SCHEMATIC BHC SONIC LOG SONDE.
COURTESY SCHLUMBERGER.

recorded simultaneously in Track 1. The interval transit time within the Taber sand has been analysed. The integrated transit time varies from 81 microseconds to 87 microseconds in oil pay sand of the Taber Mannville 'D' pool.

Determination of Porosity

After numerous laboratory experiments Wyllie (1956-58) concluded that in clean and consolidated formation with uniformly distributed small pores there is a linear relationship between porosity and transit time,

$$\Delta t_{log} = \phi \ \Delta t_f + (1-\phi) \ \Delta t_{ma}$$

or

$$\phi = \frac{\Delta t_{log} - \Delta t_{ma}}{\Delta t_f - \Delta t_{ma}}$$

where Δt_{log} = reading on the sonic log in μ sec/ft.

Δt_{ma} = transit time of the matrix material.

Δt_f = about 189 μ sec/ft (corresponding to "fluid velocity" of 5,300 ft/sec).

In the laboratory the porosity of the few core samples obtained from different boreholes within the Taber sand were determined. These core-derived porosities were plotted on abscissa against transit sonic time on ordinate in order to establish their linear relationship (Fig. 15). Δt_{ma} of sandstone from this curve was estimated at 57.4 microseconds, equivalent to a velocity of 17,500 feet/sec

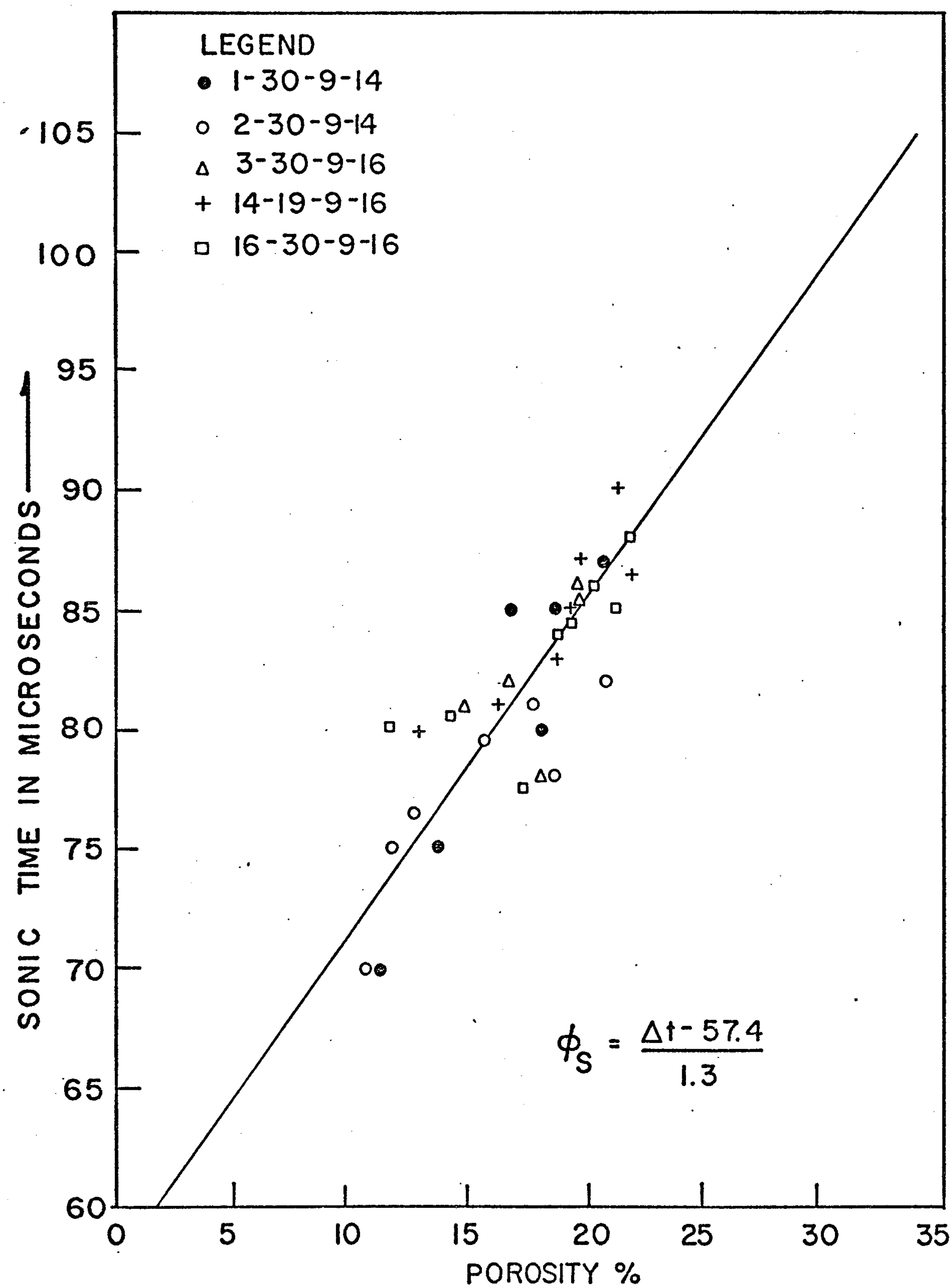

TABER D POOL, BASAL CRETACEOUS SANDSTONE

FIG.15

when porosity was considered zero. Thus log-derived porosity was converted into porosity unit by using this curve.

Formation Density Log

The formation density log responds to the electron density of the formation which is related to true bulk density, P_b, in gm/cc. The greatest accuracy is obtained when the borehole is smooth and free from mud cake. The bulk density measured by density logging device is a simple weighted average of the densities of the rock and the pore fluid. Since the lithology from core and bulk density from density log were known, the porosity was estimated from porosity-density relationship.

Principle

The schematic drawing of the dual spacing formation density logging device is shown in Fig. 16. A radioactive source, applied to the hole wall in a shielded sidewall skid, emits medium-energy gamma rays into the formation. The gamma ray rebound from the electron and give up some of its energy in a process known as Compton scattering. This process occurs most frequently when formations are bombarded with radiation in the energy range of 0.6 to 1.3 Mev. The scattered gamma rays reaching the detector, at a fixed distance from the source, are counted as an indication of formation density.

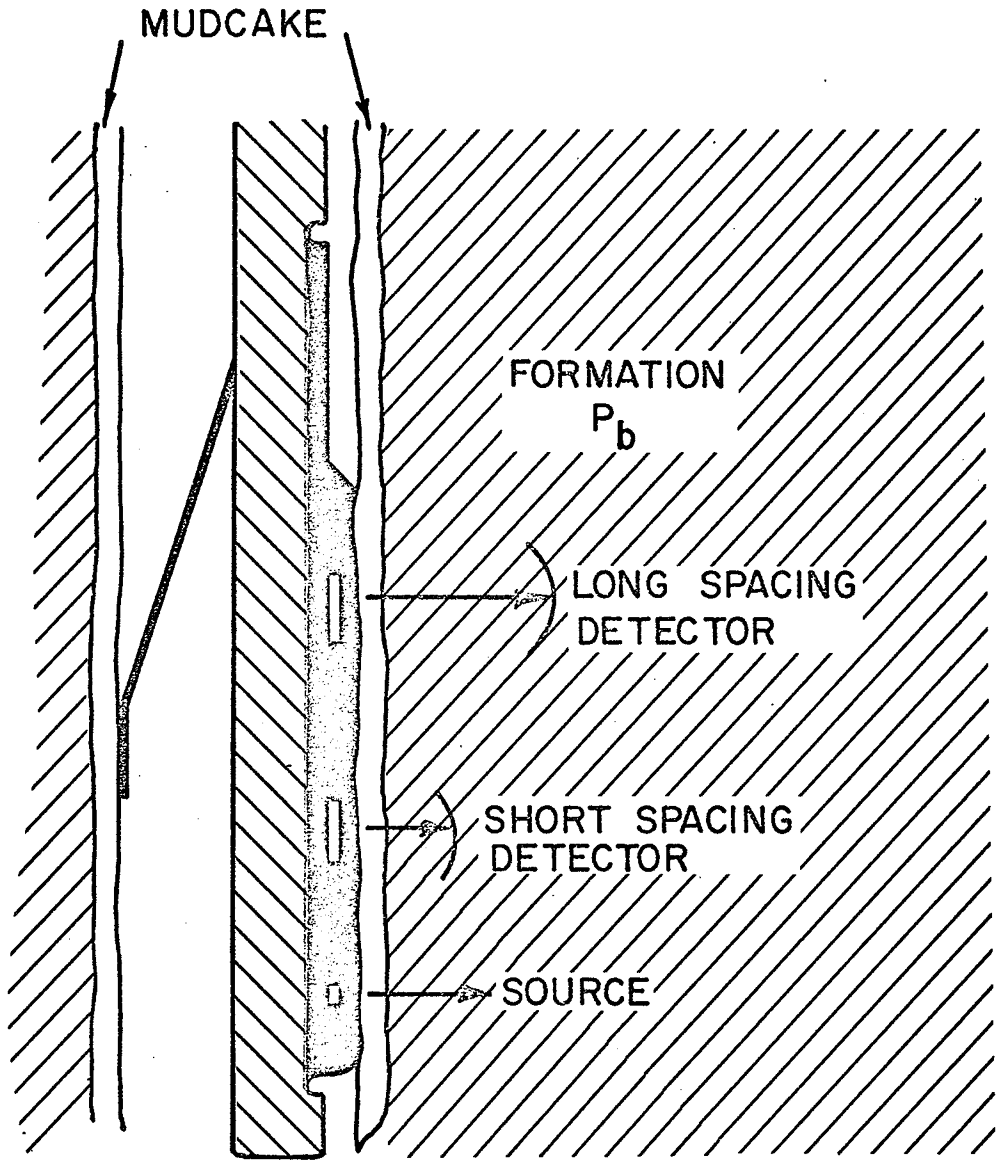

FIG.16 SCHEMATIC OF COMPENSATED DENSITY LOG SONDE.
COURTESY SCHLUMBERGER.

Equipment

Two detectors are used in the FDC (Formation Density Compensated) tool. In order to minimize the influence of the mud column, the source and the detectors, mounted on a skid, are shielded. The opening of the shield are applied against the wall of the borehole by means of eccentering the arm. A scintillation counter is used for receiving the radiation.

Log Presentation

The density log ran in the Taber sand is shown in Fig. 4. The curve has been recorded in Tracks 2 and 3 with a linear density scale in gm/cc. The gamma ray curve and the caliper have been recorded in Track 1. The bulk density of the Taber oil pay sand varies from 2.40 gm/cc to 2.45 gm/cc.

Determination of Porosity

In a clean and consolidated formation of known matrix density (ρ_{ma}) which contains a fluid of average density ρ_f; the porosity has been calculated from the equation

$$\phi = \frac{\rho_{ma} - \rho_b}{\rho_{ma} - \rho_f}$$

where ρ_b is the recorded bulk density of the formation. The relationship between bulk density and core measured porosity within the Taber sand in few wells has been established (Fig. 17). The matrix density ρ_m has been calculated 2.68 gm/cc from this relationship when porosity was considered zero.

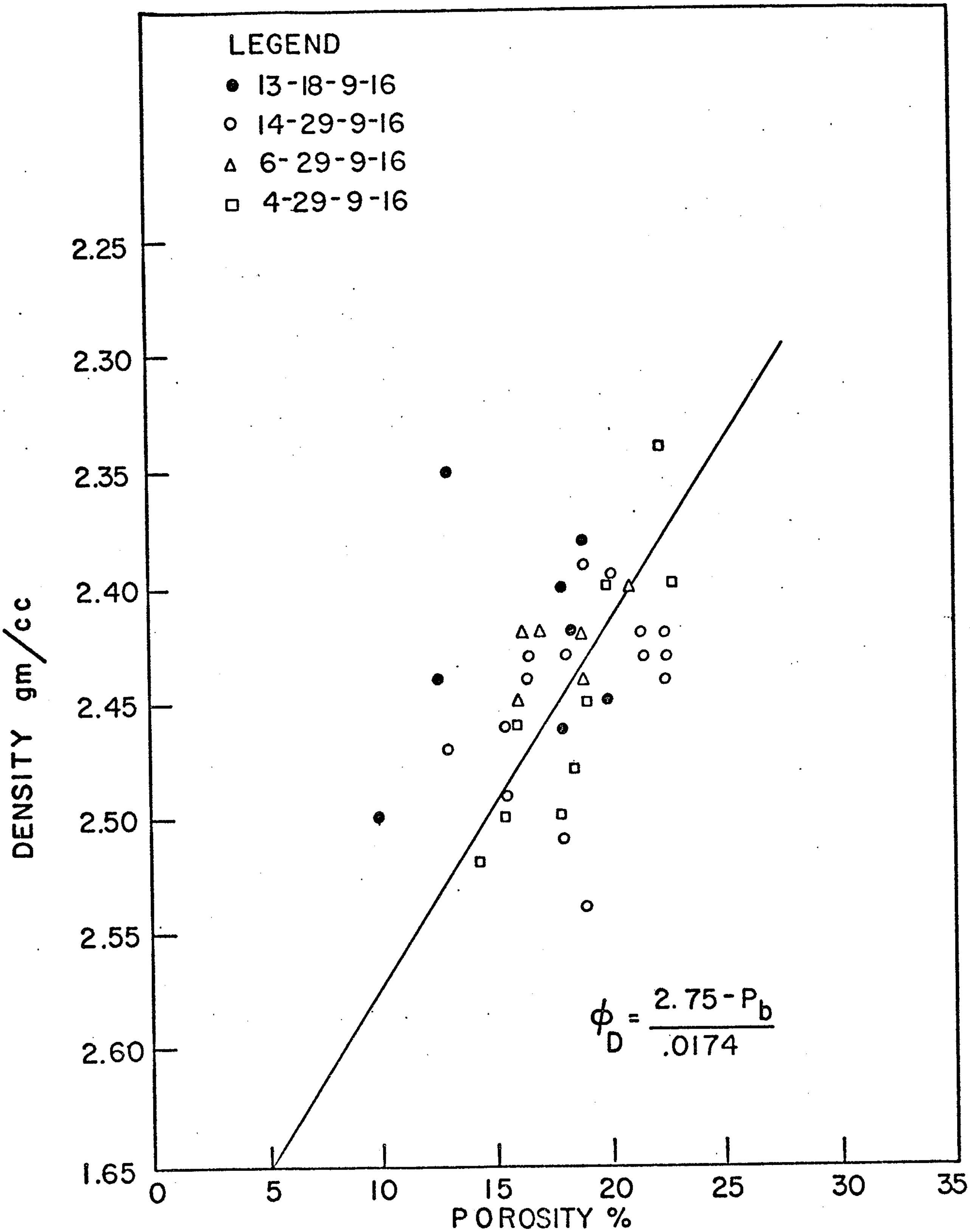

TABER FIELD D POOL, BASAL CRETACEOUS SANDSTONE

FIG.17

CHAPTER V

QUALITY OF WELL LOG DATA

Precise and dependable quantitative log analysis requires logs of best possible quality (Lynch, 1962). With the exception of few SP and induction logs obtained in dry wells during the years 1942 - 44, most of the logs in Taber Mannville 'D' pool were recorded with modern equipments from the period 1966-1971. The quality of the logs was substantially improved and the log gave more detailed information than earlier logs. No serious defects have been found in any of these logs.

An example of poor and good quality log has been shown in Fig. 18. The poor quality log was recorded with the non-focussing electrode device. The log does not permit reliable evaluation of R_t because the readings are greatly affected by the resistivity of all the media around the device (borehole, invaded and uncontaminated zone, and adjacent beds). The good quality log was obtained with Induction Electrical Survey (I-ES) tool which has a focussing device. The tool is designed in such a way that the effects of the borehole filled with fluid, the adjacent formation and the influence of invaded

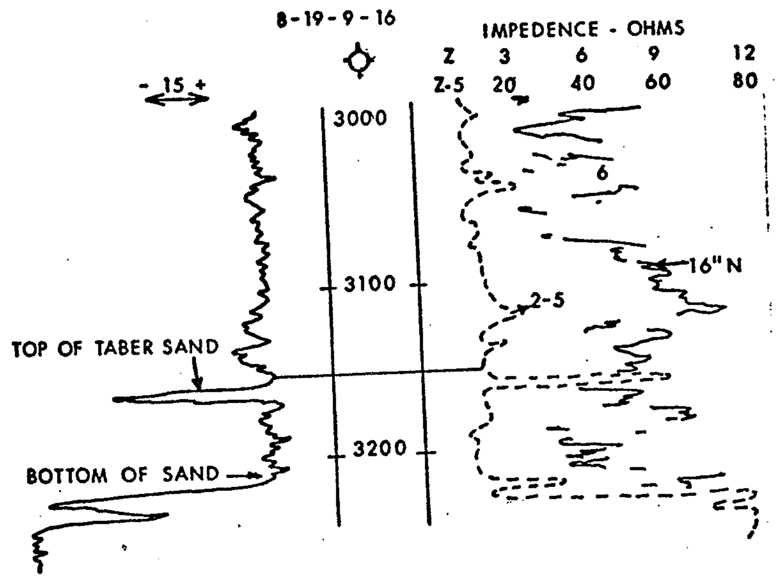

POOR QUALITY LOG RECORDED IN 1944

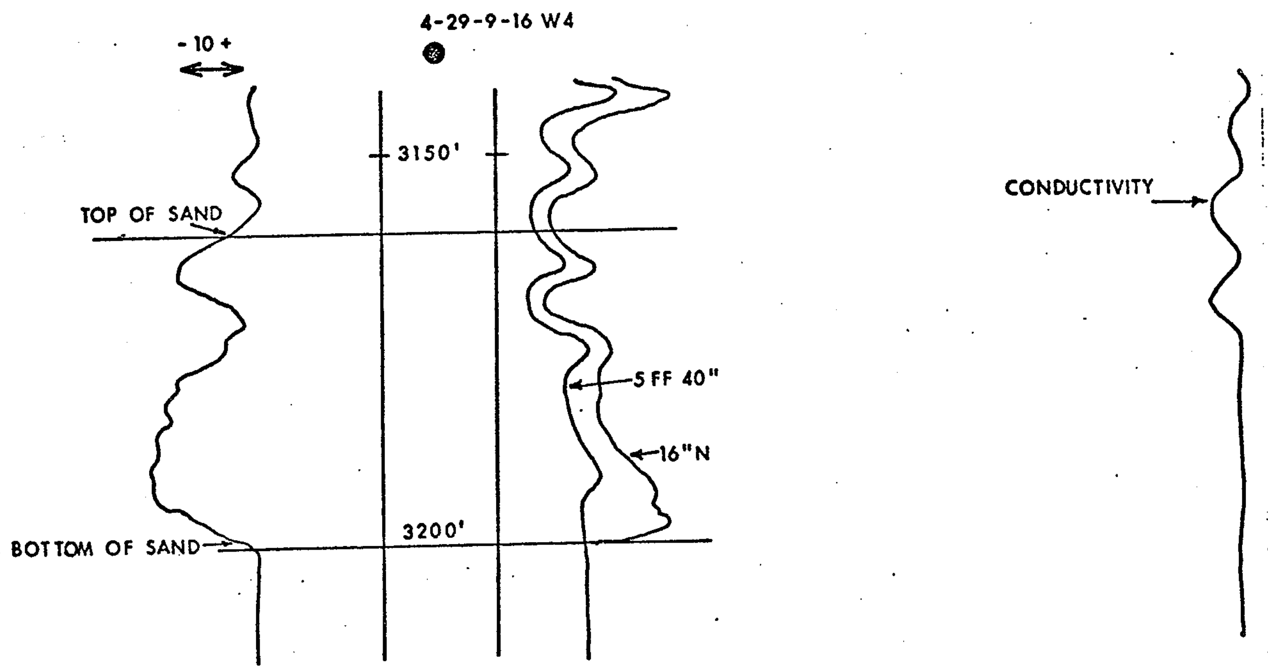

GOOD QUALITY LOG RECORDED IN 1968

FIG.18 SHOWS THE POOR AND GOOD QUALITY LOGS RECORDED IN TABER MANNVILLE 'D' POOL zone on uncontaminated zone are greatly minimized and the log furnishes good values of R_t.

CHAPTER VI

QUALITATIVE LOG INTERPRETATION

An attempt has been made to study the shapes of SP and resistivity curves qualitatively to indicate the nature of the Taber sand deposition process and to justify the use of the induction log as close to R_t. The shape of the SP curve depends on the deposition environment in which sediments are laid out. The thin fingers on the SP curves (Figs. 8 and 9) recorded within the Taber sand in some wells reflect laminations of shale within the sand as the sand becomes relatively cleaner towards the bottom of the sedimentary unit. By interpreting the sand reflections on the electrical logs it can be stated that the Taber sand is certainly sealed by relatively impervious shales. The base of the Taber sand is an erosion surface on top of Rierdon shale. The SP curve reduces to the shale base line below the top of this erosion surface. The uneven surface of the top of the Rierdon shale is interpreted as the result of differential erosion. The Taber sand overlying this erosional surface has been found to be thicker where maximum erosion took place.

The reservoir rock of Taber Mannville 'D' pool contains shale laminae which are interbedded within the sand formation. The induction log readings are not appreciably affected by the presence of these thin laminae. The induction logging was done with a focussing device and the borehole effects and adjacent formation have a negligible influence on the log reading. Thus, the resistivity value derived from the 40 in. induction log is considered very close to R_t.

The resistivity value of the Taber sand is highly variable with a maximum up to 100 ohm - meters.

The Taber sand contains two types of water;

(i) The water within the oil saturated zone is irreducible water having a resistivity of 0.15 ohm-meters as determined from an oil-base core. These waters occupy the finer pores of the sand, and

(ii) The water within the water saturated zone is fresher than the irreducible water and has resistivity variation of 1.2 ohm-meters to 1.74 ohm-meters, as established from a few water sample analyses by Atomic Absorption Spectroscopy (Macleod, 1970). This resistivity variation of formation water in Taber Mannville 'D' pool may be due to the fresh water encroachment along the Sweet Grass Arch.

CHAPTER VII

QUANTITATIVE LOG INTERPRETATION

Evaluation of Reservoir Parameter

The main physical parameters needed to evaluate a reservoir are its porosity, hydrocarbon saturation, permeable bed thickness, and permeability. These important parameters are derived or inferred from the analysis of SP, electrical induction, gamma ray, sonic, and density logs, and laboratory measurements. Quantitative analyses of these parameters involves calculations using formulae interrelating various reservoir properties and logging measurements. The equations used for quantitative log interpretation have been shown in Fig. 19.

Resistivity

Of the formation parameters obtained directly from logs, resistivity is of particular importance because it is essential to saturation determination. The resistivity of the Taber oil-pay sand which was derived directly from the 40 in. induction electrical log varies from 7 ohm-meters to 100 ohm meters. The resistivity is measured at two-foot intervals within the Taber sand

$$F = \frac{Ro}{Rw} = \frac{a}{\phi m}$$

$$Sw = \sqrt[n]{Ro / Rt} = \sqrt[n]{\frac{F\,Rw}{Rt}}$$

$$Sxo = \sqrt{\frac{F\,Rmf}{Rxo}}$$

$$Ec = -K \log_{10} \frac{Rmf}{Rw}$$

$$\Delta t \log = \phi \Delta tf + (1 - \phi)\Delta tma$$

$$\rho b = \phi \rho f + (1 - \phi) \rho ma$$

FIG. 19 BASIC EQUATIONS FOR QUANTITATIVE ANALYSIS.

from the induction electrical log.

Porosity

Porosity is the fraction of the total volume occupied by pores. It is evaluated for every two-foot interval within the Taber sand for each well, either from sonic or from density logs. The average porosity of oil pay sand is 18.9 p.c. Porosity below 17.3 p.c. is considered non-pay sand due to the low permeability of sand having porosity below this value.

Water Saturation

Water saturation, S_w, is the fraction of the pore volume occupied by formation water. The empirical relation between formation resistivity, porosity, and water saturation has been discussed in earlier chapters. For every two-foot interval within the Taber sand, water saturation is estimated by using the formula in Fig. 19. Water saturations of a few core samples were also established by laboratory measurements. The measured porosity versus measured water saturation of the core has been plotted in Fig. 20. The average porosity of 18.9 p.c. of the Taber oil pay sand corresponds to 40 p.c. water saturation in this graph which in turn gives 60 p.c. hydrocarbon saturation.

Permeability

Permeability is the measure of ease with which a

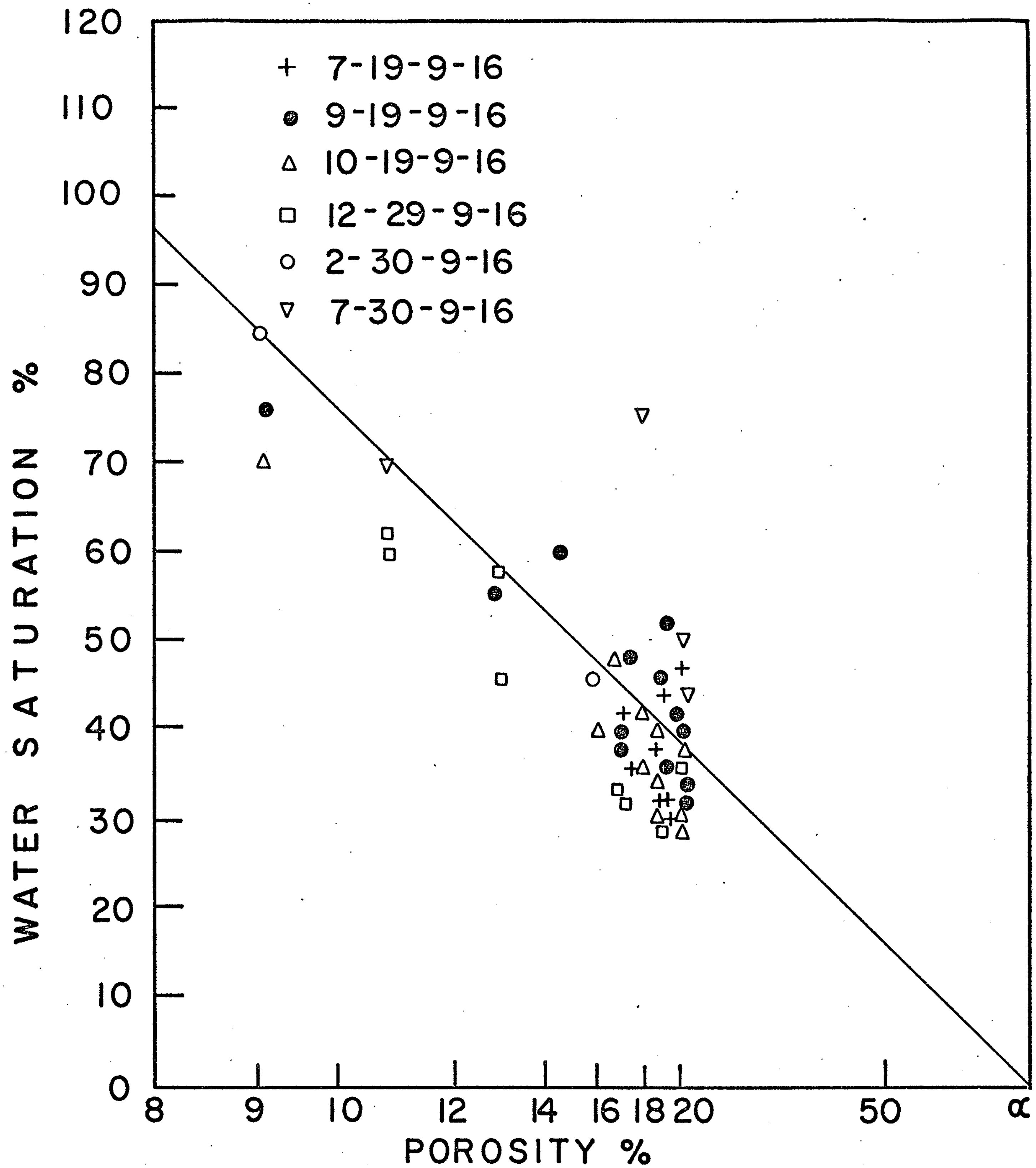

TABER D POOL BASAL CRETACEOUS SANDSTONE

FIG. 20

formation permits a fluid of given viscosity to flow through it. Permeabilities of a few core samples were determined in the laboratory by testing cores in a permeameter. The measurement is based on Darcy's law expressed by the equation

$$q = \frac{KA}{\mu} \times \frac{dp}{dx}$$

where

q = volume flux in centimeters per sec

K = the permeability constant in millidarcys

A = the cross sectional area in square centimeters

μ = the fluid viscosity in centipoises

$\frac{dp}{dx}$ = the hydraulic gradient in atmospheres per centimeter

Figure 21 shows the core-measured permeabilities plotted against core-measured porosities within the Taber sand for a few wells. The minimum porosity, 17.3 p.c., corresponds to 86 millidarcys from this curve for the oil pay sand of the Taber Mannville 'D' pool. The permeability of every two foot interval of Taber sand is determined using this curve.

Thickness of Oil Pay Sand

The thickness of formation containing hydrocarbon is needed in order to determine if the accumulation can

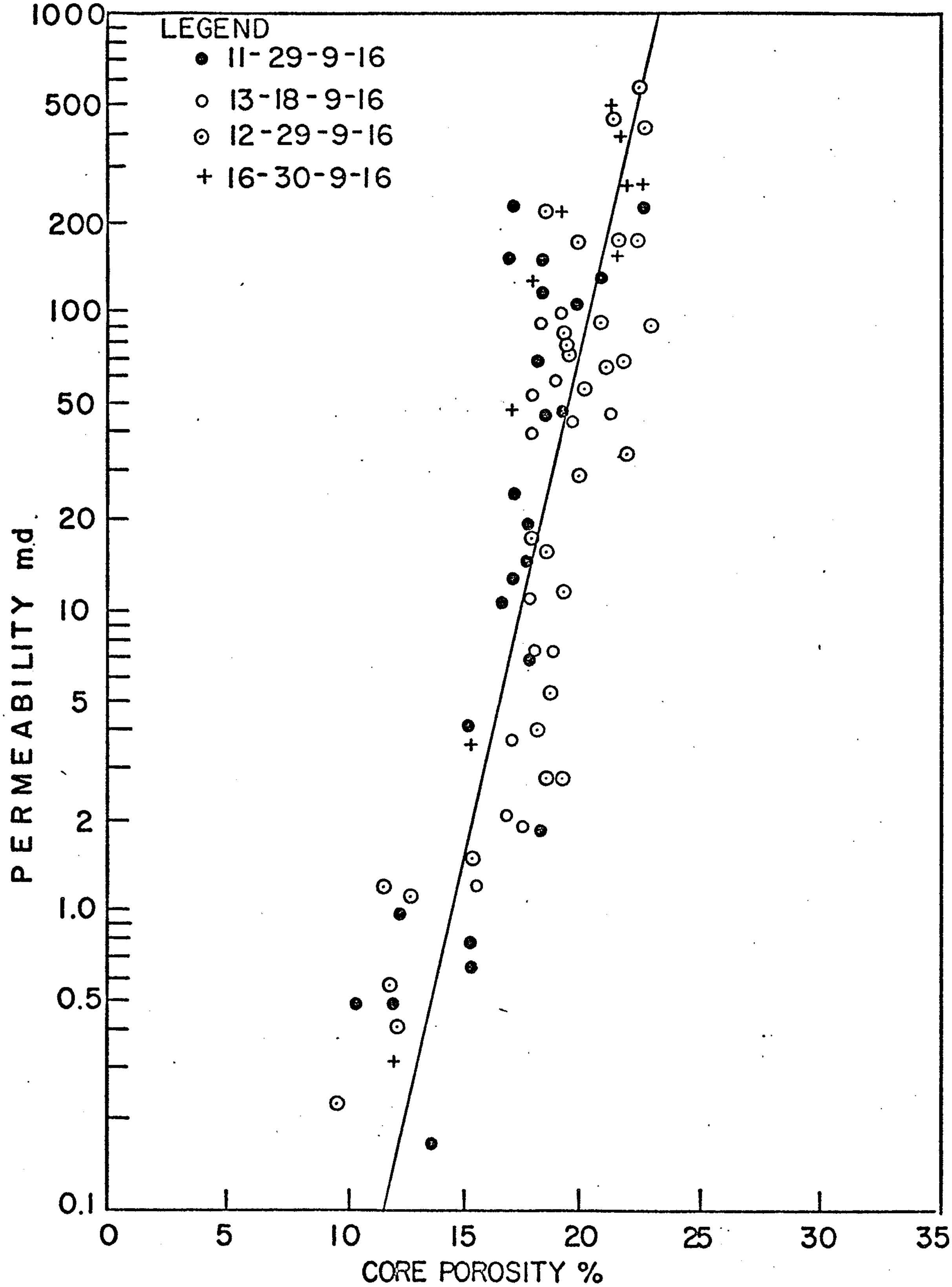

TABER FIELD D POOL, BASAL CRETACEOUS SANDSTONE

FIG. 21

be considered commercial. This has been achieved after elimination of shale streaks by gamma ray cut off of 32° API unit and non pay sand having porosity less than 17.3 p.c. which corresponds to permeability 10 millidarcys in the reservoir rock of the Taber Mannville 'D' pool. The net pay thickness varies from 2 to 46 feet.

CHAPTER VIII

RESULTS OF WELL LOG ANALYSES AND ITS TREATMENT

The results of the well log analyses are presented in the form of structure contour maps, two geologic sections, five isopach maps, an average porosity footage map and an average permeability footage map. Volumetric calculations of the pores occupied by fluid were made from the average porosity footage map and the reserve of the recoverable oil was estimated using the established reservoir parameters. A well-number index map is shown in Fig. 22.

Structure Contour Map

Figure 23 shows the structure contour on top of the bentonite marker. The top of this marker is easily recognized as it appeared as a single deflection on every SP log. The dip of the marker bed is towards the northwest. The bed is not much disturbed with an exception of minor folding in the northeast quadrant of the map.

Figure 24 shows the structure contour on top of the Taber sand. The top is recognizable on every SP log and the footage to the top of the sand is read from this log and transferred to datum (mean sea level) in feet. The

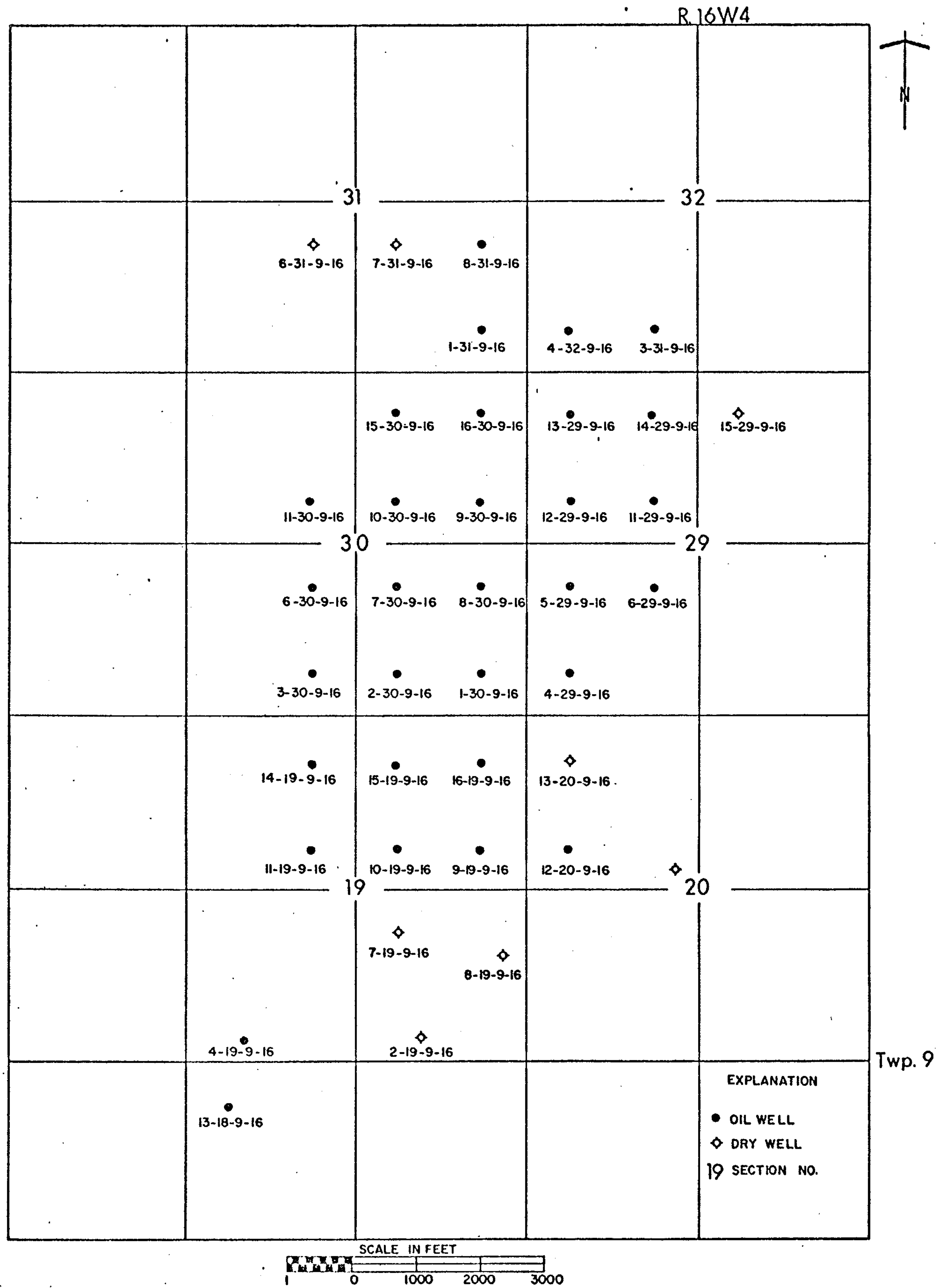

FIG.22 MAP SHOWING LOCATION OF WELLS IN Lsd., SEC, Twp., Rge., NOS IN TABER MANNVILLE 'D' POOL, TABER FIELD, ALBERTA, CANADA

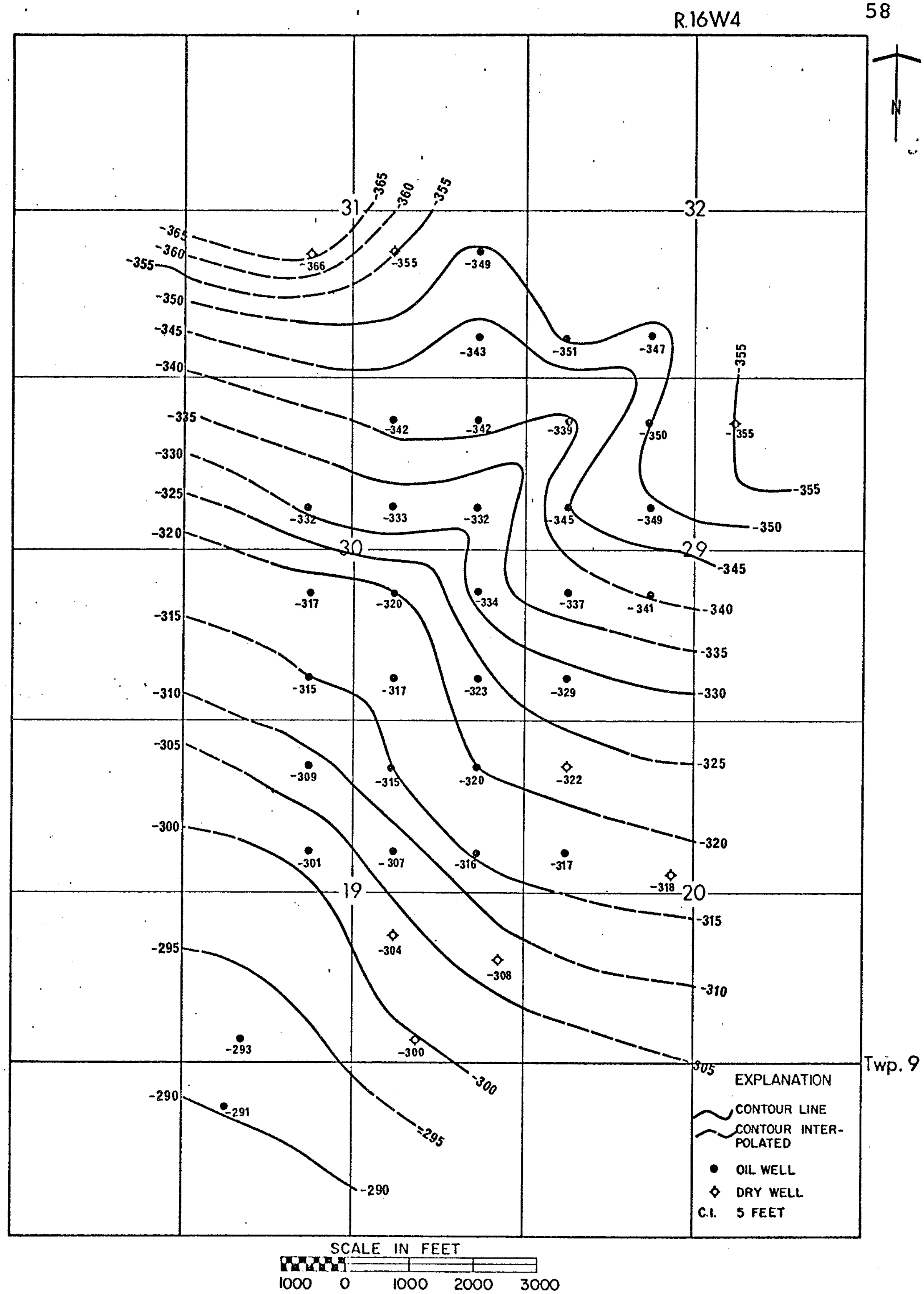

FIG.23 STRUCTURE CONTOUR ON TOP OF BENTONITE MARKER, TABER MANNVILLE 'D' POOL, TABER FIELD, ALBERTA, CANADA

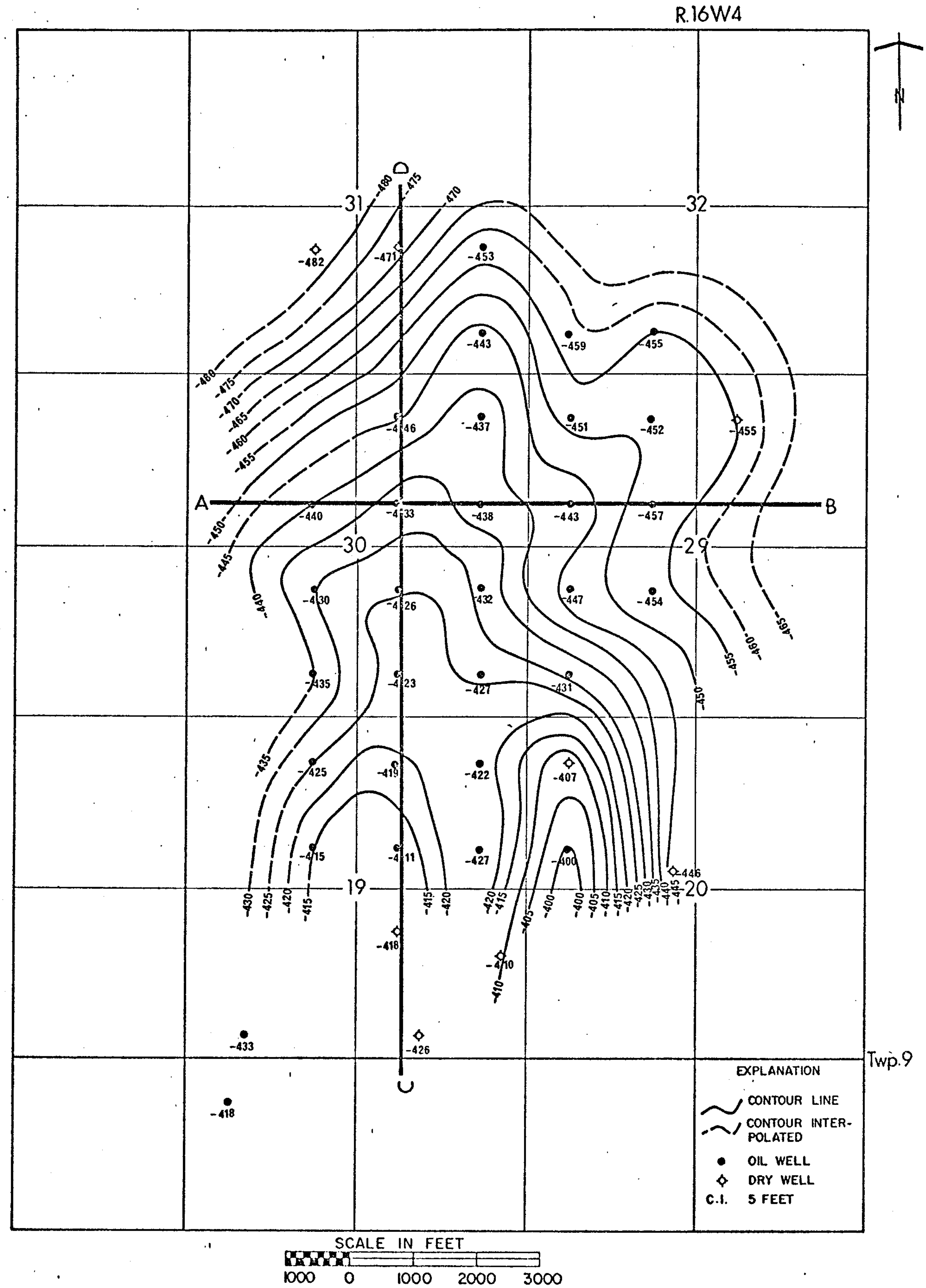

FIG.24 STRUCTURE CONTOUR ON TOP TABER SAND, TABER MANNVILLE 'D' POOL, TABER FIELD, ALBERTA, CANADA

values are plotted on the map and contoured with a contour interval of 5 feet. The top of the Taber sand deposition is irregular. A localized structural high lies in the southern part of the map. In the southeastern part there appears to be a shallow localized dome-like structure with steep gradient towards the east. To the southwest the structure is asymmetrical. There are irregular undulations in the central part of the map. To the northwest the sand deepens with a uniform gradient.

Figure 25 shows the structural contour on top of Rierdon shale. The top of the Rierdon shale is very distinct on the SP logs and the depths measured from the logs to the top of the bed was transferred to subsea level in feet and contoured at an interval of 5 feet. The general dip of the erosional surface is northwest. A minor structural deformation in the central part of this map is the result of differential erosion of the top of Rierdon shale during pre-Cretaceous time.

Geologic Section

Two geologic sections, east-west and north-south along A-B and C-D (Figs. 24 and 25) have been shown in Figs. 26 and 27. In the longitudinal section C-D (Fig. 26) which is about 3 miles long, the sand body is decidedly arched in the middle of the section, with each end of the section lower than the middle. The base of the sand slopes

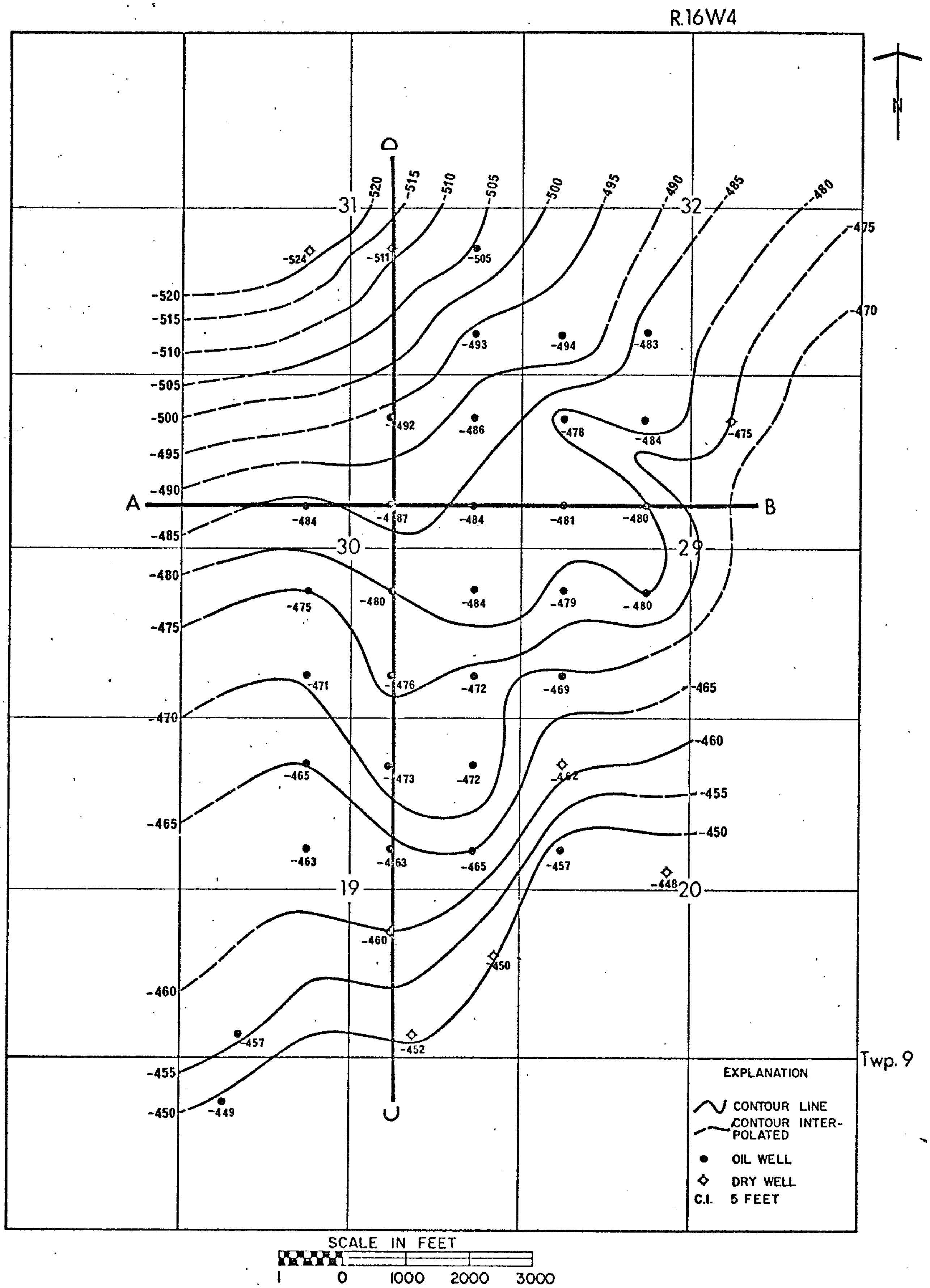

FIG.25 STRUCTURE CONTOUR ON TOP OF RIERDON SHALE TABER MANNVILLE 'D' POOL, TABER FIELD, ALBERTA, CANADA

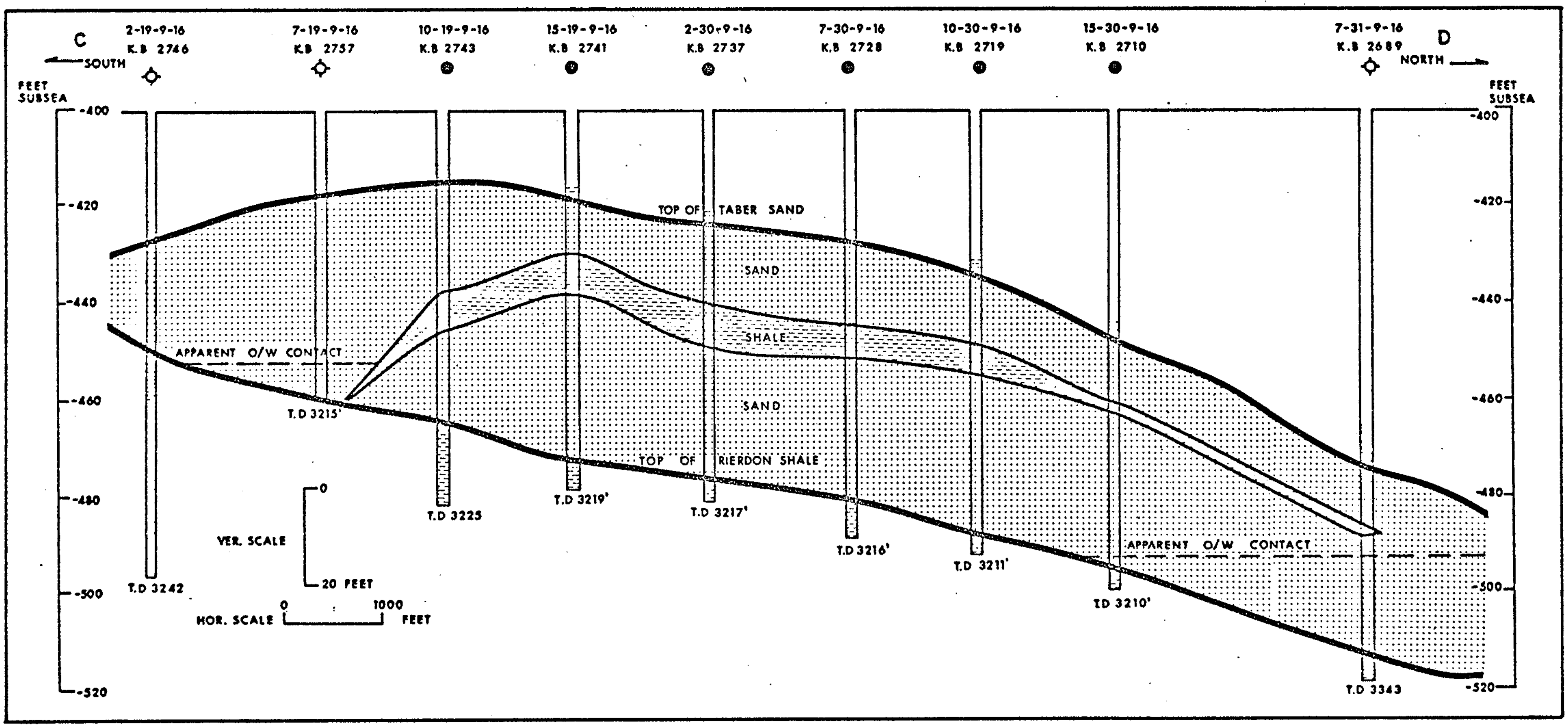

FIG.26 TABER SAND STRATIGRAPHIC TRAP DELINEATED ACROSS C-D (SEE FIG.24), TABER MANNVILLE 'D' POOL, TABER FIELD, ALBERTA, CANADA

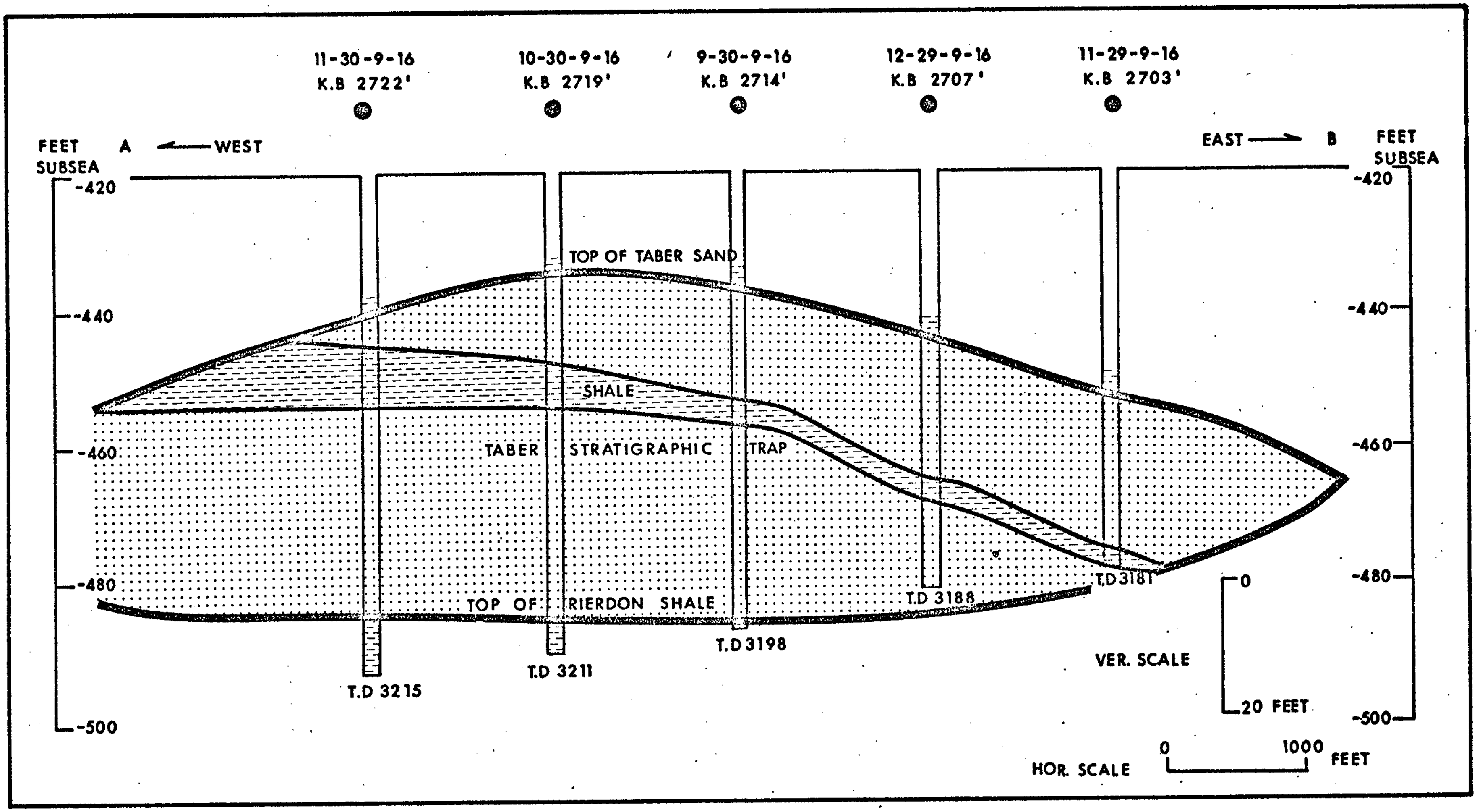

FIG. 27 TABER SAND STRATIGRAPHIC TRAP DELINEATED ACROSS A-B (SEE FIG. 24)
TABER MANNVILLE 'D' POOL, TABER FIELD, ALBERTA, CANADA

gradually towards the north and the rapid sloping of the upper surface may indicate pinch-outs of the sand towards north within a short distance. The upper surface of the sand is concave down.

Nine wells along this section penetrated the entire Taber sand. Out of these nine wells drill stem test (DST) recovered oil from five wells and water and oil from three wells. The apparent water oil contact has been marked in three wells based on the results of drill stem test. The water oil contact in the southern well is at different elevation below sea level than that northern well and the migration of water and oil has been restricted by the presence of interbedded shale within the reservoir rock.

The interbedded shales have been correlated with the results obtained partly from core analyses and partly from the recognition of characteristic gamma ray curve opposite to shale. The other section A-B (Fig. 27) is at right angles to C-D and much shorter. The sand pinches rapidly in the east. The upper surface of the sand is also concave down. Along this section three wells out of five penetrated the entire Taber sand. All of the five wells are oil producing. Drill stem test (DST) recovered only oil and no water from any of these wells.

Isopach Map

Five isopach maps (Figs. 28 to 32) have been prepared in order to find out the shape, extension and inferred origin of Taber sand. The net oil pay map may also be used for volumetric calculation of hydrocarbon fluid in Taber Mannville 'D' pool.

Figure 28 shows the isopach of the interval between the bentonite marker and top of the Rierdon shale. The map shows the thinning of intervening sediments towards the east. The thinning may have been caused due to lesser supply of sediments during deposition on the surface of Rierdon shale. The thickening to the west may be the result of relatively more deposition of sediments in this direction.

Figure 29 shows the isopach of the interval between the bentonite marker and the top of Taber sand. As expected the Taber sand in parts of the Sections 19 and 20 indicates a thinning of the interval because differential compaction occurred, thus permitting a thicker accumulation of shale around the sand lens.

The map of Fig. 30 is an isopach of the interval between the top and bottom of the Taber sand. The map feature supports a thicker Taber sand development in Section 19 and this has been confirmed by drilling location in Lsd. 10, Sec. 19, Twp. 9, Rge. 16, W4Me (Fig. 22). The Taber sand body is lenticular in shape and

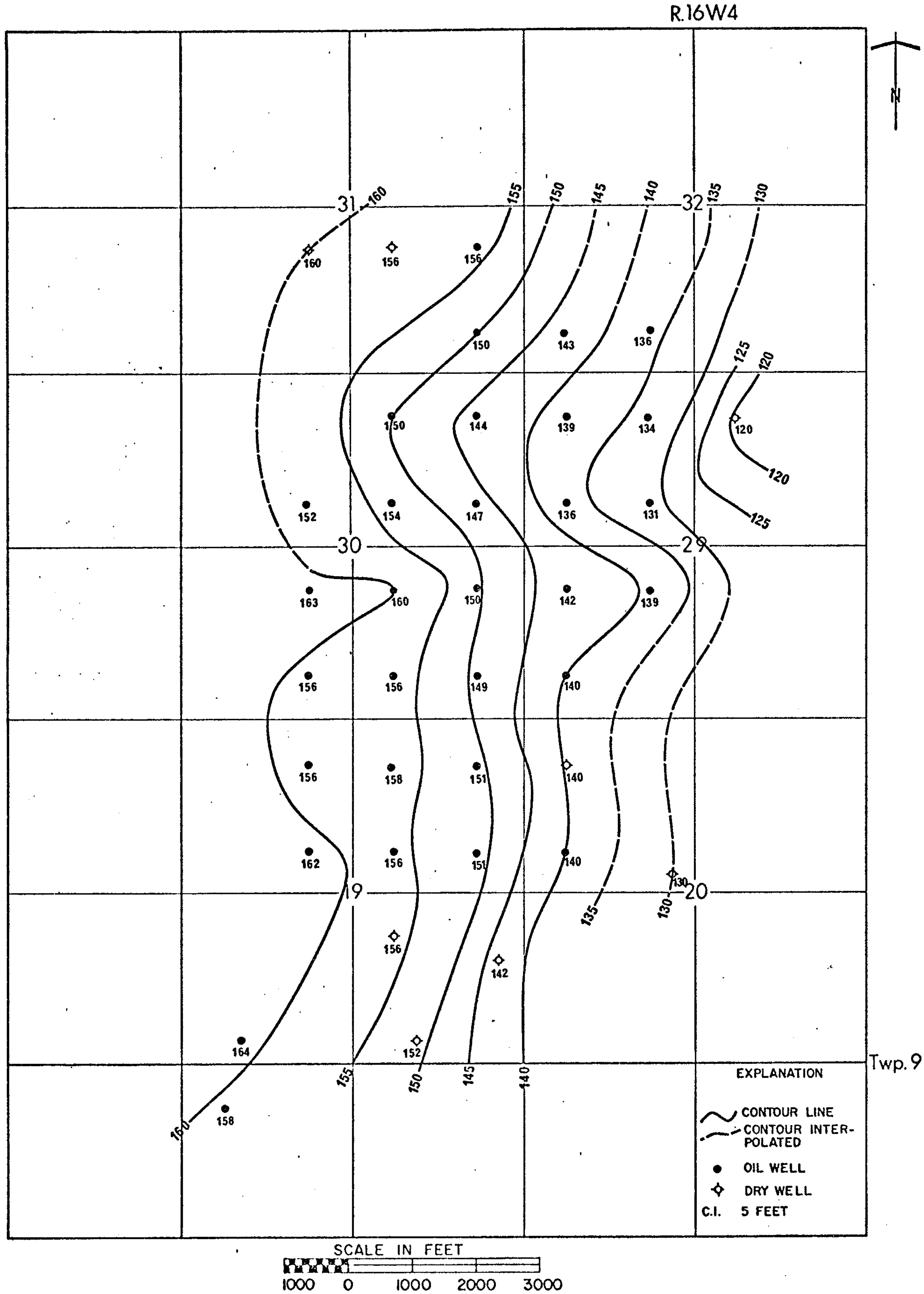

FIG. 28 ISOPACH MAP BENTONITE MARKER AND RIERDON SHALE, TABER MANNVILLE 'D' POOL, TABER FIELD, ALBERTA, CANADA

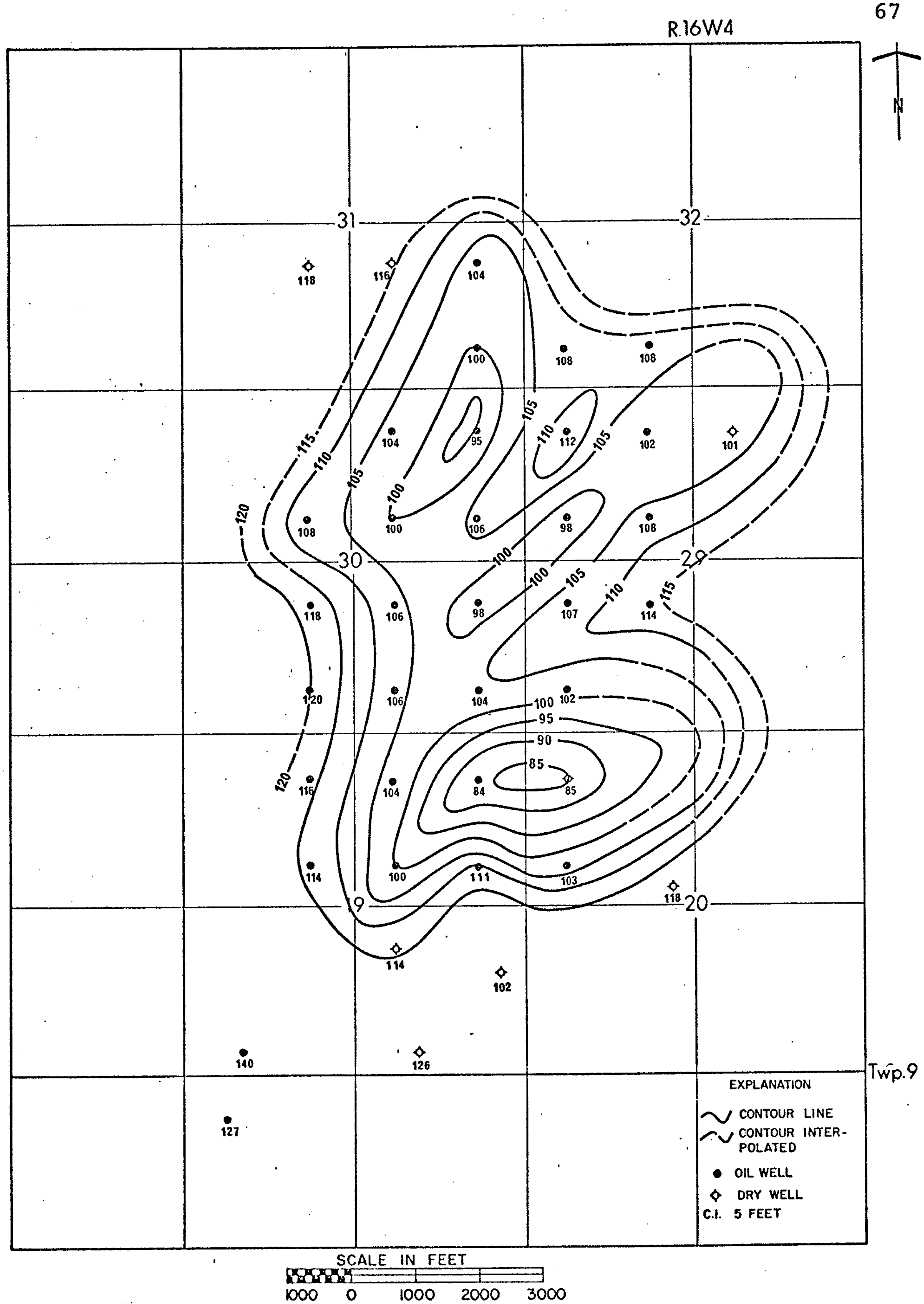

FIG.29 ISOPACH MAP BENTONITE MARKER AND TOP OF TABER SAND, TABER MANNVILLE 'D' POOL,

TABER FIELD, ALBERTA, CANADA

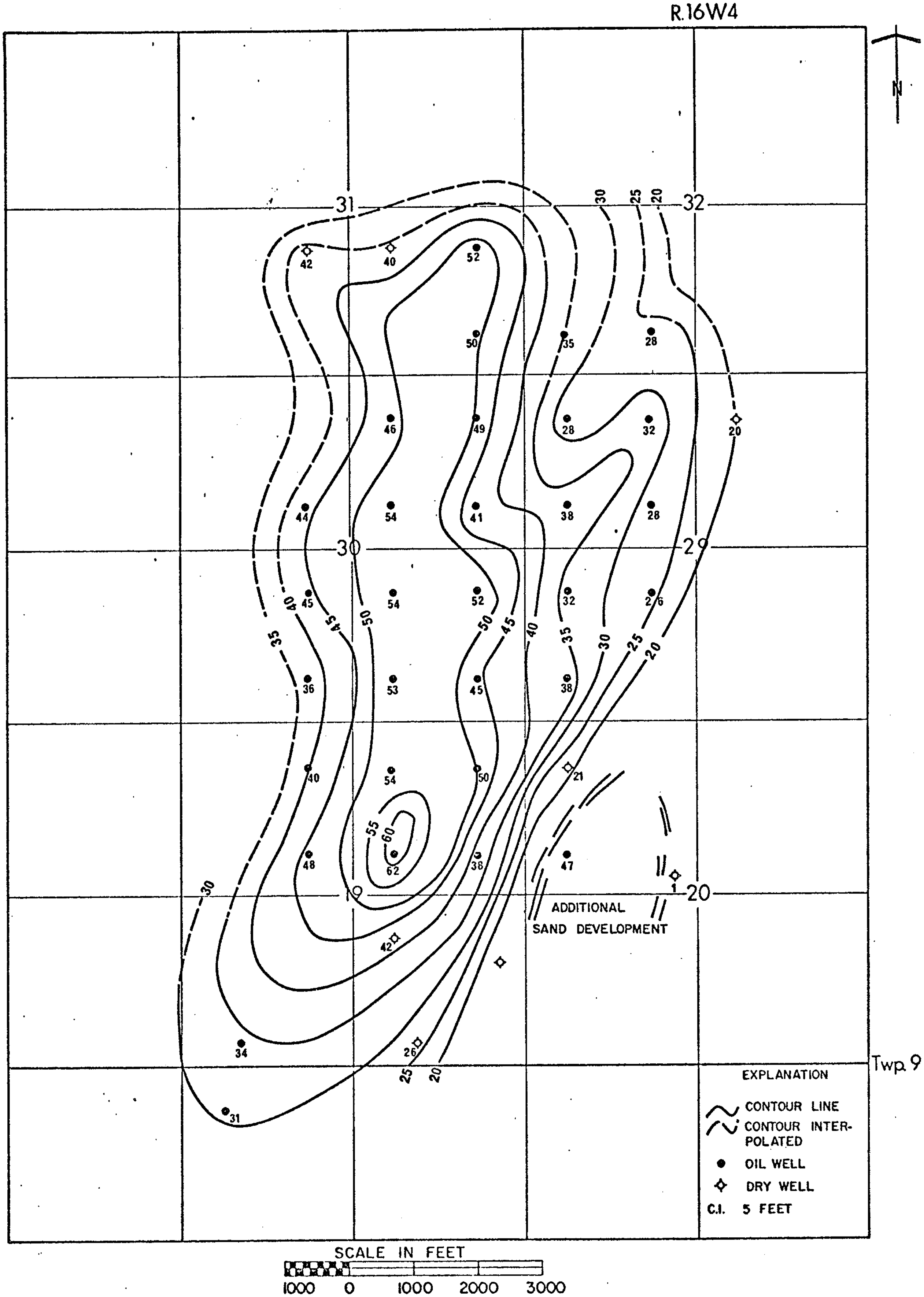

FIG.30 ISOPACH MAP TABER SAND, TABER MANNVILLE 'D' POOL, TABER FIELD, ALBERTA, CANADA

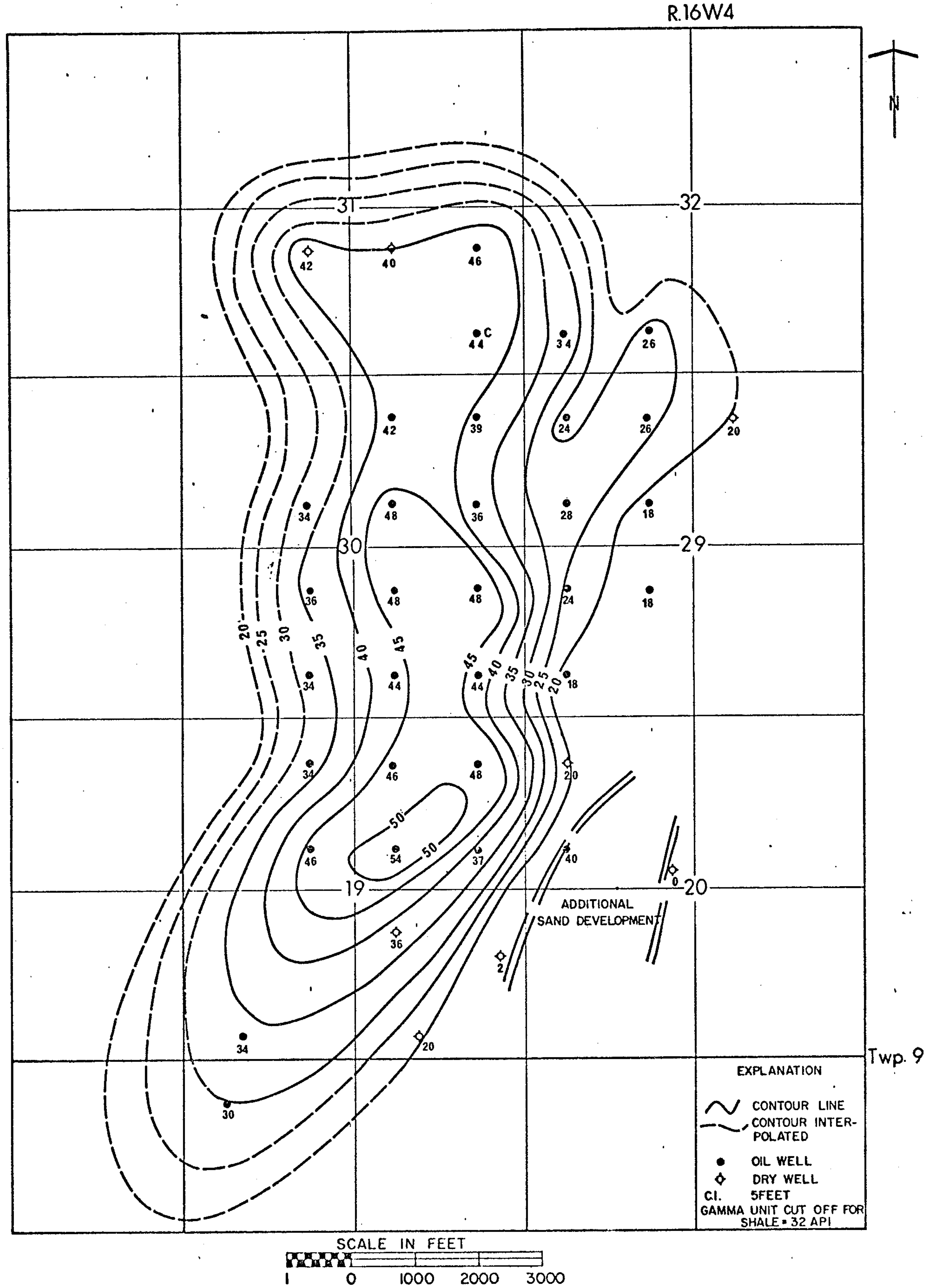

FIG.31 ISOLITH NET SAND MAP, TABER MANNVILLE 'D' POOL, TABER FIELD, ALBERTA, CANADA

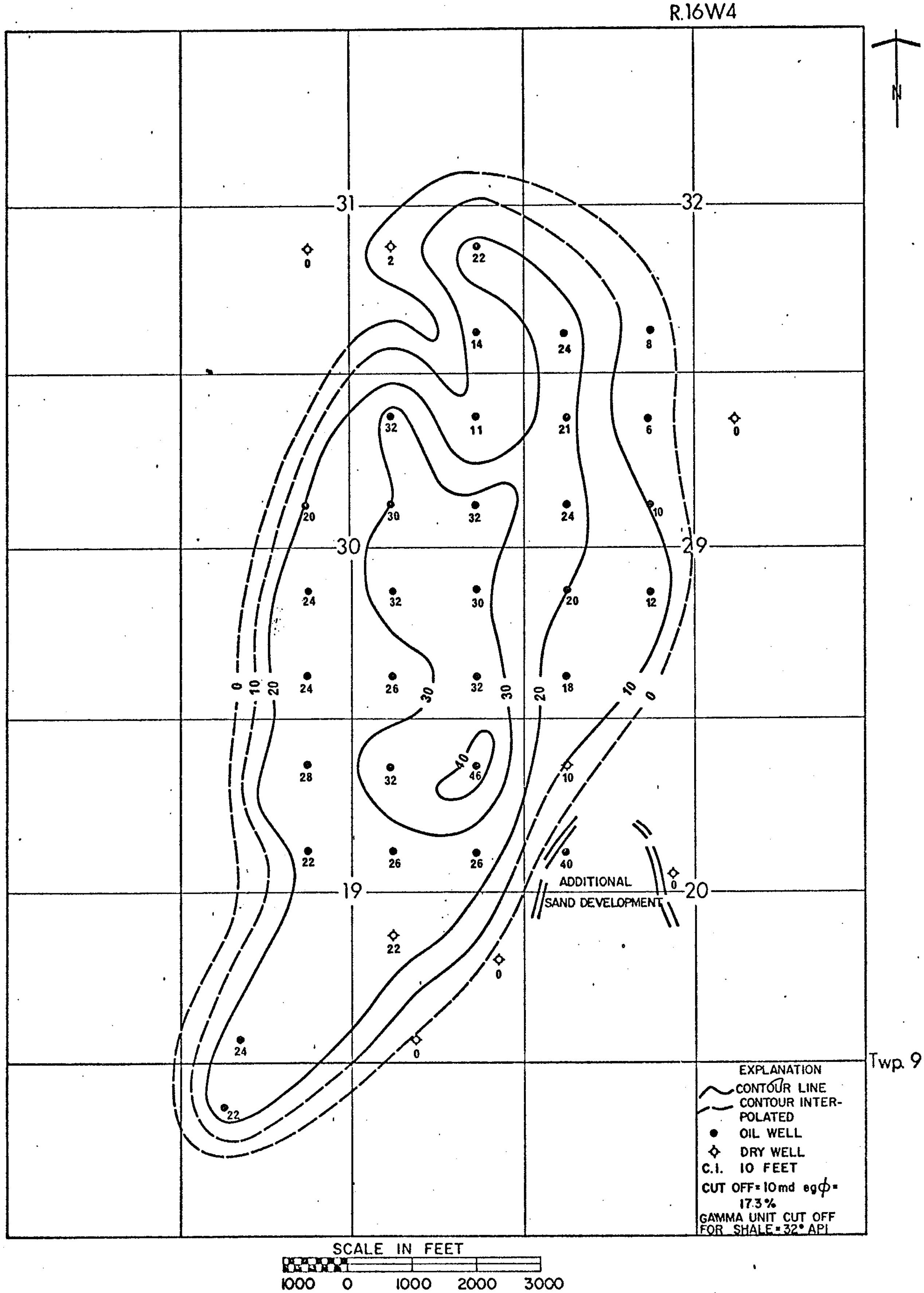

FIG.32 NET PAY MAP OF TABER SAND, TABER MANNVILLE 'D' POOL, TABER FIELD, ALBERTA, CANADA

extended in a north-south direction. The trap is due to the lenticular pinch of the sand across a plunging structure.

Figure 31 shows the isolith net-sand map. The objective of making this map is to see the change in shape of the Taber sand body after eliminating the interbedded shale within the reservoir rock. The pattern of the sand body remains almost identical as the previous map (Fig. 30). The gamma-ray value of 32° API units was used as the shale cutoff in preparing this map.

The net pay map of the Taber sand is shown in Fig. 32. The portion of the Taber sand having porosity less than 17.3 p.c. (equivalent permeability of 10 millidarcys) are considered non-pay sands in making this map. The pool has been outlined and its periphery is enclosed by the zero contour. The maximum thickness of oil-pay sand is 46 feet.

Porosity Footage Map

The average porosity footage map is shown in Fig. 33. The map has been prepared for use in the volumetric calculation of pores which are occupied by irreducible water and hydrocarbon fluid. The average porosity of net pay sand within the individual well is known from log analyses and this is multiplied by the pay thickness. The values are then plotted on the map and contoured at an interval of 2.000 porosity footage unit. In the volumetric

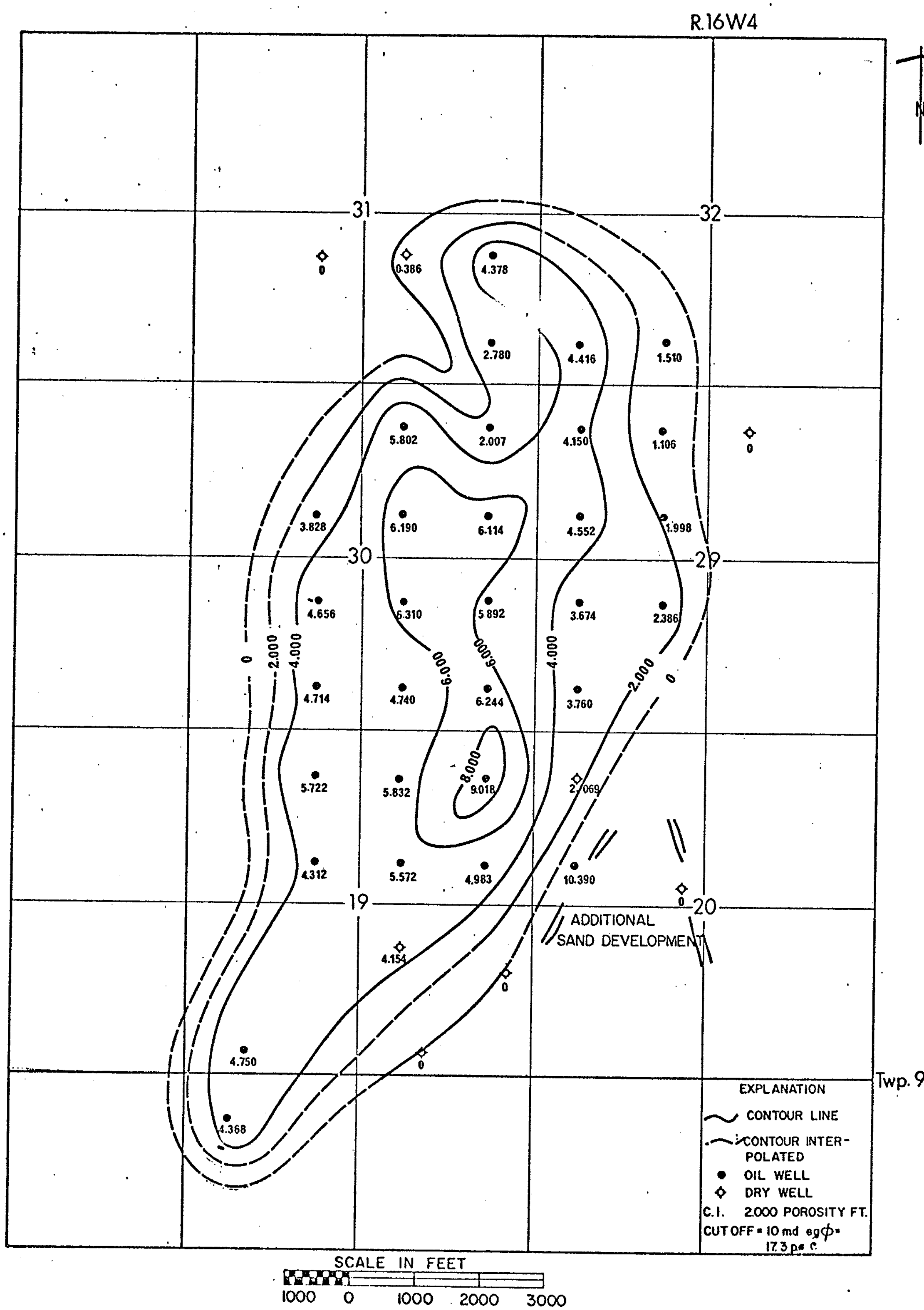

FIG.33 AVERAGE POROSITY FOOTAGE MAP TABER MANNVILLE 'D' POOL, TABER FIELD, ALBERTA, CANADA

calculations the area contained within any enclosure are measured by planimeter. The volume calculated is the sum of the area enclosed by two adjacent contours times one-half the contour interval. The total volume of the pores occupied by fluid has been estimated 6369.90 acre-feet.

Permeability Footage Map

The permeability footage map has been shown in Fig. 34. The map is prepared to find out the area of highest capacity of fluid flow. The average permeability of net pay sand within individual well is calculated from the porosity-permeability relationship established in Fig. 21. The average permeability is then multiplied by net pay thickness and plotted on the map. The figures are contoured at an interval of 650 permeability footage units. Two areas of high capacities can be seen in Sections 19 and 30 and a capacity barrier exists along the periphery of dry wells.

Estimation of Total Recoverable Oil

One of the most important aspects of well log analyses is to estimate the total recoverable oil from the Taber Mannville 'D' pool. This involves primary and secondary factors, shrinkage factor and other important reservoir parameters such as average oil saturation, average porosity and thickness of the pay which are estimated out of well log analyses. The primary recovery

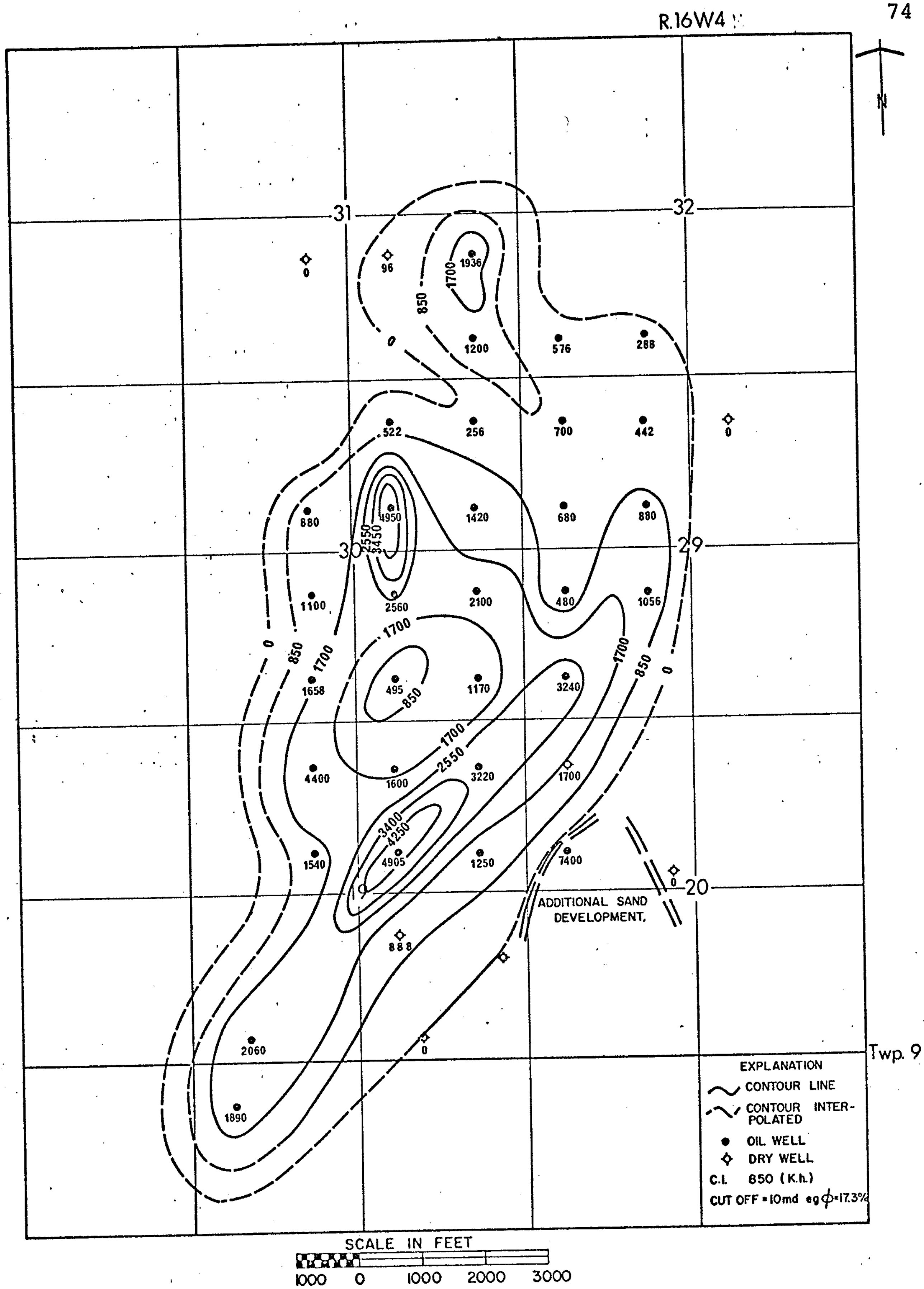

FIG.34 CAPACITY (KH) IN OIL PAY SAND, TABER MANNVILLE 'D' POOL, TABER FIELD, ALBERTA, CANADA

factor 5 p.c., secondary recovery factor 12 p.c., and shrinkage factor 95.8 p.c. were established by the production section, Chevron Standard Limited, Calgary, for Taber Mannville 'D' pool. The total recoverable oil is thus estimated in the following processes.

Total oil reserve = 7758 x (Avge. porosity
x Avge. pay thickness
x area in acres)
x Avge. oil saturation
x shrinkage factor

where the figure 7758 is the number of barrels of oil in acre per foot when porosity is 100 p.c.

The sum of the product of the factors within the bracket is estimated from the average porosity footage map of Fig. 31.

Thus the total oil reserve = 7758 x 6369.90 x $(I-S_w)$
x 0.95
= 7758 x 6369.90 x 0.60
x 0.95
= 28.25 million barrels

Primary recovery = 28.25 x 0.05
= 1.41 million barrels

Secondary recovery = 28.25 x 0.12
= 3.39 million barrels

Total recoverable oil = 1.41 + 3.39
= 4.80 million barrels

CHAPTER IX

DISCUSSION OF THE RESULTS

The Taber sand body is underlain and overlain by shales and varies considerably in thickness even within the small area of the proven pool. Shale streaks are interbedded within the reservoir rock as confirmed in a number of drilling wells. The oil reservoir is a medium- to fine-grained sand within shale formation of Lower Cretaceous age. Examination of two cores under microscope (See Appendix II and III) disclose that the colour of the reservoir rock is light grey to dark grey with some black streaks. The porosity is intergranular and the permeability is reduced by the presence of shale streaks within the reservoir rock. The interbedded sandstone and shale contains numerous carbonized laminae, streaks of coal and prints of plant leaves which are evidence of the non-marine deposition of the Lower Cretaceous Mannville Group in the area of study.

In order to determine the origin of the Taber sand deposit, it was important to consider the shape of the sand body and the sizes of its constituent minerals. Cross sections of the Taber sand bodies do not show the shape of a deep channel with steep sides, or with a fairly level top and rounded or pointed bottom as we would expect in filling of stream channels. The sand bodies are lenticular in shape and are surrounded by shales which may have been the source rock. The pattern and shape of the lens, their double convex cross sections and its fine- to medium-grained constituents suggest that the Taber member is a sand bar. The bar has a long axis of approximately 14,000 feet and an average width of approximately 4,000 feet. The base of the bar is relatively flat, while the top is convex. The bar is a separate and sealed reservoir.

The Taber sands are the products of depositional environment. The trap formed into the reservoir rock is a stratigraphic one which has been completely isolated due to lenticular pinch-out of sand which results in an isolated zone of porosity and permeability. In the two geologic cross sections the dip of the top of Taber sand body does not conform in a general way with the dip on the top of Rierdon shale. In both the cross sections the sand bodies are thick in the middle and thin out at the ends. Structure as represented by Rierdon shale and top of Taber sand does not seem to conform, hence there appears to be no relation between the Taber sand deposits, structure of the top of Rierdon shale and the accumulation of oil in the reservoir rock. Since the Taber sand bodies are lenticular in shape, they themselves form structural highs, which are excellent reservoirs for the accumulation of oil. The oil in the reservoir probably originated very close to where it is found, the shales which enclose the sand lens being the source rock. The compacting forces exerted during the period of probable differential settling literally may have squeezed the oil with connate water, from its source to sand reservoir around which the settling took place.

CHAPTER X

CONCLUSIONS

The well log analyses of 38 wells in Taber Mannville 'D' pool delineate the stratigraphic trap which was formed in fine- to medium-grained sand reservoirs of Lower Cretaceous age. The sand body is lenticular in shape, surrounded by shales which may have been the source rock, and is an excellent oil reservoir. The pattern and shape of the sand lens, its excellent sorting and the lithology of the enclosed shales suggest that the Taber member is a sand bar. The sand deposit has no relation to the structure as represented by the top of Rierdon shale. The bodies themselves form a structural high for the accumulation of oil. An average porosity of 18.9 p.c., an average permeability of 86 millidarcys and an average water saturation of 40 p.c. have been estimated for the oil pay sands of the Taber Mannville 'D' pool. The total recoverable oil has been estimated as 4.80 million barrels out of 28.25 million barrels of oil in place. The oil has a gravity of 18.6° API.

REFERENCES

Andrichuk, J.M.
1970. Facies analysis of Upper Devonian Wabamun Group in West Central Alberta, Canada. Bull. A.A.P.G. v. 44, No. 10, pp. 1651-1681.

Archie, G.E.
1942. The electrical resistivity log as an aid in determining some reservoir characteristics. Pet. Tech., v. 5, No. 1.

Cheyney, A.E.
1948. Madison Shoestring Pool, Greenwood County, Kansas. A.A.P.G., v. 11, pp. 150-159.

Doll, H.G. and Martin, M.
1960. Electric log combinations and improved interpretation. Geophysics, v. 25, No. 4, pp. 854-882.

Glaister, R.P.
1959. Lower Cretaceous of Southern Alberta and adjoining areas. Bull. A.A.P.G., v. 43, No. 3, pp. 590-640.

Hage, C.O. and Hume, G.S.
1941. The geology of East Central Alberta. G.S.C. Mem. 232, pp. 11-15.

Hume, G.S.
1928. Oil and gas in Western Canada. G.S.C. Eco. Geo. Series, No. 5.

Kokesh, F.P. and Blizard, R.B.
1959. Geometric factors in sonic logging. Geophysics, v. 24, No. 1, pp. 64-76.

Landes, K.K.
1951. Petroleum Geology. Chapman and Hale Ltd., London.

Levorsen, A.I. (ed.)
1941. Possible future of oil province of the United States and Canada. Bull. A.A.P.G., August, pp. 1-154.

Levorsen, A.I.
1954. Geology of Petroleum. Tulsa, Oklahoma.

Lowenstam, H.A.
1948. Marine Pool, Madison County, Illinois, Silurian Reef producer. A.A.P.G., v. III, pp. 153-188.

Lynch, E.J.
1962. Formation Evaluation. Harper's Geoscience Series, Harper and Row.

MacLeod, W.G.
1970. AAS data from Taber-Bantry area, southern Alberta. Chevron Standard Limited.

Moran, J.H. and Kunz, K.S.
1962. Basic theory of induction logging. Geophysics, v. XXVII, No. 6, pp. 829-858.

Pickell, J.J. and Heacock, J.G.
1960. Density Logging. Geophysics, v. XXV, No. 4, pp. 891-904.

Pirson, S.J.
1970. Geologic Well Log Analysis. Gulf Publishing Company, Houston, Texas.

Robert, D.C.
1948. Long Beach Oil Fields, Los Angeles County, California, Structure of Typical American oil fields. A.A.P.G., v. II, pp. 63-74.

Russell, L.S. and Landes, R.W.
1940. Geology of the southern Alberta plains. G.S.C. Mem. 221,

Schlumberger Well Survey Corporation
1958. Introduction to Schlumberger Well Logging, No. 8.

1969. Log Interpretation Principle.

1969. Schlumberger Log Interpretation Charts.

Sheriff, R.E.
1970. Glossary of terms used in well logging. Geophysics, v. 35, No. 6, pp. 1116-1139.

Tixier, M.P. Alger, R.P. and Tanguy, D.R.
1960. New development in induction and sonic logging. Jour. Pet. Tech., v. 12, No. 5.

Wyllie, M.R.J., Gregory, A.R. and Gardener, G.H.F.
1956. An experimental investigation of factors affecting elastic wave velocities in porous media. Geophysics, v. 21, No. 1, pp. 41-70.

Wyllie, M.R.J.
1960. Log interpretation in sandstone reservoirs. Geophysics, v. XXV, No. 4, pp. 748-778.

APPENDICES

Appendix I - Generalized table of formations in southern plains of Alberta, Canada.

Era	Period or Epoch		Group or Formation	Lithology
Cenozoic	Recent and Pleistocene			River gravels, sand and tills, etc.
	Pliocene			Clay, sandstone
	Oligocene		Cypress Hills	Conglomerate, sandstone silts, marl and gravel
	Upper Paleocene		Ravenscrag	Predominantly sandstone and clay
	Lower Paleocene			Clay, soft sandstone
Mesozoic	Cretaceous	Upper	White Mud	Sandstone, silt and clay
			East End	Silt, sand and shale
			St. Mary River	Alternate sandstone and shale, lignite
			Blood Reserve	andstone
			Bearpaw	Shale and bentonite
			Old Man	Shale, coal and bentonite
			Foremost	Shale, lignite, silt Clay and bentonite
			Pakowki	Shale, sandy shale and sandstone
			Milk River	Predominantly shale and sandstone
			Alberta	Predominantly shale and sandstone
		Lower	Bow Island	Predominantly shale
			Mannville (Taber, cutbank, sunburst)	Principally greenish and reddish shale, sandstone near the base
	Jurassic		Ellis (Rierdon)	Predominantly shale
Paleozoic	Mississippian		Rundle	Limestone, partly dolomite and cherty in place
			Banff Exshaw	
	Devonian			Predominantly limestone and shale
	Cambrian?			Predominantly limestone and dolomite, shale, etc.

Appendix II - Analyses of core of oil well in Lsd.4, Sec. 29, Twp. 9, Rge. 16 W4Me

Core No.	Formation	Depth Interval in Ft.	Lithology
1	Lower Cretaceous	3159-61	Calcareous light sands with clay in fill, light grey coloured and fine-grained sand
		61-67	Porosity high. Medium grey coloured sand with clay in fill.
		67-76.5	Very fine grained. Completely interbedded in calcareous shale matrix. Light grey colour with laminated shale interbedded. Numerous cross-bedding.
		76.5-95	Brown, very fine, clean frosted green, subangular to subrounded non calcareous clay in fill. Fair porosity with oil stain and bleeding.
		95-97	Calcareous fine-grained sand with the clay in fill.
		97-3200	Calcareous fine-grained sand.
		3200-3200.5	Apple green compacted shale.

Appendix III - Analysis of core of dry well in Lsd. 11, Sec. 20, Twp. 9, Rge. 16 W4Me

Core No.	Formation	Depth Interval in feet	Lithology
#1, 3109-3129 Recovery 19'6"	Lower Cretaceous Ellis Madison	12'5"	Dark grey silty shale with scattered ironstone concretion
		3'	Very compacted fine grained shaly sandstone, slight calcareous and grey in colour.
		3'	Dark grey shale with streak of coal at the top
		1'	Fine grained grey coloured sandstone with numerous carbonized laminae
#2, 3129-3149 Recovery 18'10"		7'	Fine grained sandstone and interbedded with silty shale with streaks of ironstone slightly calcareous.
		3'	Cross bedded sandstone with few ironstone concretion, fine grained, dark coloured.
		8'10"	Shale and sandstone interbedded with streaks of ironstone with numerous carbonized plant remains.
#3, 3149-3169 Recovery 21'6"		2'7"	Dark grey, fine-grained silty shale Fine to medium grained sandstone with plant remains calcareous and compacted sandstone.
		12'6"	Dark grey silty shale with scattered pyrite laminae and plant leaves print clear at the bottom.

Core No.	Formation	Depth Interval in feet	Lithology
#4, 3169-3174 Recovery 3'1"	Top of Taber Sand at 3169'	1'6"	Medium-grained calcareous sandstone with intergranular porosity. Dark coloured oil stained sandstone. Grains are rounded. Bottom sharp contact with Ellis shale.
	Top of Ellis at 3172'9"	1'3"	Green pyrite shale.
#5, 3190-3210 Recovery 12'7"	Belemnite zone at 3200'	10'	Calcareous green shale.
	Top of basal Ellis sand at 3201'	1'	Green shaly calcareous sand, chert, pebbles at top.
		1'	White quartzose fine to medium grained sand.
		7"	Sand with spotty oil staining, good intergranular porosity.
#6, 3210-24 Recovery 5'4"	Ellis-Madison contact at 3220'	4'	Calcareous medium grained white quartzose, glauconite sand with good porosity.
		1'4"	Contact is sharp, grey massive cherty dolomite with less porosity.

Appendix IV - Well Compilation Sheet, Taber Mannville 'D' Pool Taber Field, Alberta, Canada.

Well	Location	K.B.	T.D.	Status	Log Available	Core	(1) Top of Taber sand in feet	(2) Bottom Taber Sand in feet
Chevron Taber	13-18-9-16W4th.	2756.7'	3208'	●	density, I.E.S.	3178-3164=66 3184-3208=24	-418	-449
Taber C.P.R.	2-19-9-16W4th.	2746	3242	✧	electrical	nil	-426	-452
Chevron Taber	7-19-9-16W4th.	2750.3	3215	✧	sonic, I.E.S.	3162-3213=51	-418	-460
Taber C.P.R.	8-19-9-16W4th.	2740	3252	✧	electrical	nil	-410	-450
Anadarko Taber	9-19-9-16W4th.	2744	3220	●	sonic, induction	3150-3208= rec. 58	-427	-465
Anadarko Taber	10-19-9-16W4th.	2743	3225	●	I.E.S., sonic	3155-3215= rec. 60	-411	-473
Anadarko Taber	11-19-9-16W4th.	2747	3220	●	sonic, I.E.S.	3156-3167=11 3167-3180=13 3180-3210=35	-415	-463
Anadarko Taber	14-19-9-16W4th.	2747	3217	●	I.E.S. density sonic, gamma	nil	-425	-465
Anadarko Taber	15-19-9-16W4th.	2741	3219	●	sonic, I.E.S.	3156-3214= rec. 58	-419	-473
Anadarko Taber	16-19-9-16W4th.	2736	3218	●	I.E.S., sonic	3145-3169=24 3169-3208=39	-422	-472
Taber Province	11-20-9-16W4th.	2722	3236	✧	electrical	nil	-446	-448
Chevron Taber	12-20-0-16W4th.	2737.1	3190	●	I.E.S., density	3137-3190= rec. 39	-400	-447
Chevron Taber	13-20-9-16W4th.	2732.2	3276	✧	density log, induction log	3142-3202= rec. 55	-407	-428
Chevron Taber	4-29-9-16W4th.	2728.7	3207	●	density, I.E.S.	3159-3202= rec. 41.5	-431	-469
Chevron Taber	5-29-9-16W4th.	2718.7	3199	●	I.E.S., density	3154-3199= rec. 45	-447	-479[c]
Chevron Taber	6-29-9-16W4th.	2711.7	3198	●	density, I.E.S.	3160-3197=37	-454	-480
Rozsa Taber	11-29-9-16W4th.	2703	3183	●	sonic, I.E.S.	3152-3183=31	-457	-480
Rozsa Taber	12-29-9-16W4th.	2707	3188	●	I.E.S., sonic	3138-3188=51	-443	-481[c]
Well Spruce Dalex Taber	13-29-9-16W4th.	2697	3168	●	Gamma ray, I.E.S.	nil	-451	-478
Rozsa Taber	14-29-9-16W4th.	2696	3187	●	I.E.S., sonic	nil	-452	-484
Rozsa Taber	15-29-9-16W4th.	2693	3250	✧	I.E.S.	nil	-455	-475
Anadarko Taber	1-30-9-16W4th.	2733	3215	●	Sonic, I.E.S.	3158-3206=48	-427	-472
Chevron Taber	4-19-9-16W4th.	2753.4	3276	●	dual induction sonic density gamma log	3172-3218=46	-433	-457
Anadarko Taber	2-30-9-16W4th.	2737	3217	●	sonic, I.E.S.	nil	-423	-476
Anadarko Taber	3-30-9-16W4th.	2741	3217	●	I.E.S., sonic	3158-3205=47	-435	-471
Anadarko Taber	6-30-9-16W4th.	2734.4	3213	●	sonic, I.E.S.	3150-3183=33 3184-3201=17 3201-3207=6	-430	-475
Anadarko Taber	7-30-9-16W4th.	2728	3216	●	I.E.S., sonic	3172-3211=39	-426	-480
Anadarko Taber	8-30-9-16W4th.	2722	3210	●	I.E.S., sonic	3156-3203	-432	-484
Rozsa Taber	9-30-9-16W4th.	2714	3198	●	I.E.S., sonic	nil	-438	-479
Rozsa Taber	10-30-9-16W4th.	2719	3211	●	sonic, I.E.S.	nil	-433	-487
Anadarko Taber	11-30-9-16W4th.	2722	3215	●	sonic, I.E.S.	3153-3169=16 3169-3205=36	-440	-484
Rozsa Taber	15-30-9-16W4th.	2710	3210	●	I.E.S., sonic	nil	-446	-492
Spruce Dalex Taber	16-30-9-16W4th.	2703	3173	●	Gamma-collar log	3140-3173=33	-437	-486
Spruce Dalex Taber	1-31-9-16W4th.	2695	3187	●	I.E.S., sonic	nil	-443	-493
Canadian Pacific Oil & Gas Barn	6-31-9-16W4th.	2686.4	3283	●	sonic, I.E.S.	nil	-482	-524
Home Majestic Mine	7-31-9-16W4th.	2689	3343	✧	I.E.S., micro log	nil	-471	-511
Joe Phillips Taber	8-31-9-16W4th.	2685	3195	●	I.E.S., sonic	nil	-453	-505
Joe Phillips Taber	3-32-9-16W4th.	2691	3180	●	sonic, I.E.S.	nil	-455	-483
Spruce Dalex Taber	4-32-9-16W4th.	2687	3162	●	I.E.S., sonic	3112-3162=50	-459[c]	-494[c]
Anadarko Taber	7-7-10-16W4th.	2663	3508	✧	I.E.S., sonic	nil	-497	-513

Well	(3) Thickness Taber Sand (ft)	(4) Top of Bentonite Marker (ft)	(5) Thickness Bentonite, Erosional Surface =(2-4) in ft	(6) Thickness of Upper Marker to Top of Taber =(1-4)in ft	(7) Thickness Porous Sand (ft)	(8) Net Pay Thickness Porous Sand (ft)	(9) Average Porosity in p.c.	(10) Average Porosity x footage
Chevron Taber	31	-291	158	127	30	22	19.8	436.8
Taber C.P.R.	26	-300	152	126	20	0	-	0
Chevron Taber	42	-304	156	114	36	22	18.9	415.4
Taber C.P.R.	45	-308	142	102	2	0	0	0
Anadarko Taber	38	-314	151	111	37	26	19.2	498.3
Anadarko Taber	62	-307	156	100	54	26	21.4	557.2
Anadarko Taber	48	-301	162	114	46	22	19.6	431.2
Anadarko Taber	40	-300	156	156	34	28	20.4	572.2
Anadarko Taber	54	-315	158	104	46	32	19.4	583.2
Anadarko Taber	50	-320	151	84	48	46	19.6	901.8
Taber Province	2	-318	130	128	0	0	0	0
Chevron Taber	47	-317	150	103	40	40	20.9	1039.0
Chevron Taber	21	-322	144	85	20	10	20.6	206.0
Chevron Taber	38	-329	140	102	30	18	20.8	376.0
Chevron Taber	32[c]	-337	142	107	24[c]	20[c]	18.4[c]	367.4
Chevron Taber	26	-341	139	114	18	12	19.9	238.6
Rozsa Taber	23	-349	131	108	18	10	19.9	198.8
Rozsa Taber	38[c]	-345	136	98	38	24	18.9	455.2
Well Spruce Dalex Taber	28	-339	139	112	24	21	19.8	415.0
Rozsa Taber	32	-350	134	102	26	6	18.4	110.6
Rozsa Taber	20	-354	128	101	20	0	0	0
Anadarko Taber	45	-323	149	104	44	32	19.5	624.4
Chevron Taber	24	-293	164	140	34	24	19.8	485.0
Anadarko Taber	50	-317	156	106	44	26	18.2	474.0
Anadarko Taber	36	-315	156	120	34	24	19.6	471.4
Anadarko Taber	45	-317	163	118	36	24	19.4	465.6
Anadarko Taber	54	-320	160	106	48	32	19.7	631.8
Anadarko Taber	52	-334	150	98	48	30	19.6	589.2
Rozsa Taber	41	-332	147	106	36	32	19.1	611.4
Rozsa Taber	54	-333	154	100	48	30	20.6	619.0
Anadarko Taber	40	-332	152	108	34	20	19.1	382.8
Rozsa Taber	46	-342	150	104	38	32	18.1	580.2
Spruce Dalex Taber	49	-342	144	95	39	11[c]	18.4[c]	200.7
Spruce Dalex Taber	50	-343	150	100	44	14	19.8	278.0
Canadian Pacific Oil & Gas Barn	42	-364	160	118	42	0	0	0
Home Majestic Mine	40	-355	156	116	40	2	19.3	38.6
Joe Phillips Taber	52	-349	156	104	46	22	19.9	437.8
Joe Phillips Taber	28	-347	136	108	26	8	18.9	151.0
Spruce Dalex Taber	35[c]	-351	143	108	34[c]	24[c]	18.4[c]	441.6
Anadarko Taber	16	-375	138	122	16	0	0	0

Well	(11) Pore Volume Weighed Porosity x Footage	(12) Median Permeability x footage	(13) Average Permeability in m.d.	(14) Permeability x footage	(15) Drill Stem Test (D.S.T.)
Chevron Taber	435.6	1892.0	86	1890.0	3145-3184=39', rec. 300'oil, 120'mud, 240'water
Taber C.P.R.	0	0	0	0	No D.S.T.
Chevron Taber	435.6	1892.0	40	880.0	3170-3215=45', rec. 440' blk oil, 1540' water
Taber C.P.R.	0	0	0	0	3147-3174=27', rec. 150' gassy oil
Anadarko Taber	514.8	2236.0	48	1250.0	3150-3211=61', rec. 240' oil, 576' water
Anadarko Taber	514.8	2236.0	190	4905.0	3153-3225=72', rec. 573' m.c. oil
Anadarko Taber	435.6	1892.0	70	1540.0	3172-3193=21', rec. 124', g.c. oil, 185 gas, 409' water
Anadarko Taber	554.4	2408.0	157	4400.0	3166-3218=52', rec. 150' O.C.M., 300 oil, 480' water
Anadarko Taber	633.6	2752.0	50	1600.0	3154-3219=65, rec. 1110' GSY SLI MCO, 90' O.C.M.
Anadarko Taber	910.8	3956.0	70	3220.0	3124-3218=94', rec. 950' G & M.C.O., 30' G & O.C.M.
Taber Province	0	0	0	0	No. D.S.T.
Chevron Taber	792.0	3440.0	185	7400.0	3127-3190=63', rec.60' oil, 390' mud, 120' muddy water
Chevron Taber	198.0	860.0	170	1700.0	3135-3202=67', rec. 180' drilling mud
Chevron Taber	356.4	1548.0	180	3240.0	3143-3207=64', rec. 1010 oil, 160' O.C.M.
Chevron Taber	396.0	1720.0	24	480.0	3168-3199=31', rec. 650 cln oil
Chevron Taber	237.6	1032.0	88	1056.0	3155-3198=43', rec. 150' mud, 700' oil
Rozsa Taber	198.0	860.0	88	880.0	3155-3183=28', rec. 532' oil, 180' O.C.
Rozsa Taber	475.2	2064.0	36	680.0	3148-3188=40', rec. 1886' oil
Well Spruce Dalex Taber	415.0	1800.0	86	700.0	3108-3168=58', rec. 1100' oil, 60' O.C.H.
Rozsa Taber	118.8	516.0	24	442.0	3148-3187=39', rec. 120' GSY mud cut oil
Rozsa Taber	0	0	0	0	No. D.S.T.
Anadarko Taber	633.6	2752.0	60	1170.0	3157-3215=58', rec. 582' M.C.O., 58' O.C.M.
Chevron Taber	485.0	2060.0	86	2060.0	3186-3200=14', rec. 100' mud cut oil, 700' oil, 320' only water, 620' water
Anadarko Taber	514.8	2236.0	19	495.0	3152-3215=63', rec. 1150' oil
Anadarko Taber	475.2	2064.0	70	1658.0	3152-3215=63', rec. 1150' oil
Anadarko Taber	475.2	2064.0	50	1100.0	3150-3213=63', rec. 200' cln oil, 245 M.C.O., 240' O.C.M.water
Anadarko Taber	633.6	2752.0	80	2560.0	3149-3216=67', rec. 60' Hvy O.C. Mud, 800' M.C.O.
Anadarko Taber	594.0	2580.0	70	2100.0	3121-3206=85', rec. 480' oil, 180 O.C.M.
Rozsa Taber	633.6	2752.0	44	1420.0	3145-3193=48', rec. 1550' oil
Rozsa Taber	594.0	2580.0	165	4950.0	3151-3211=60', rec. 1335' oil, 20' mud
Anadarko Taber	396.0	1720.0	44	880.0	3142-3215=73', rec. 172' M.C.O., 100' O.C.M.
Rozsa Taber	633.6	2752.0	16	522.0	3155-3210=55', rec. 32' oil, 245' O.C.M.C.W.
Spruce Dalex Taber	217.8	946.0	24	254.0	3143-3173=30', rec. 850' oil
Spruce Dalex Taber	278.0	1200.0	86	1200.0	3130-3170=40', rec. 335' oil, 150' O.C.M.
Canadian Pacific Oil & Gas Barn	0	0	0	0	No D.S.T.
Home Majestic Mine	19.8	39.6	49	96.0	3178-3183=5', rec. 20' O.C. Mud, 1680' oil
Joe Phillips Taber	435.6	1892.0	88	1936.0	No. D.S.T.
Joe Phillips Taber	158.4	688.0	36	288.0	No. D.S.T.
Spruce Dalex Taber	475.2	2064.0	24	5576.0	3135-3162=27', rec. 850'clean oil, 20' mud
Anadarko Taber	0	0	0	0	3440-3495=55', rec. 240' muddy O.C.W., 940' O.C.